COMPUGUT

An in silico tool for investigating the colon-diet-flora system

Eberl Computational Biomathematics Laboratory
University of Guelph, Guelph, Ontario, Canada

User Documentation

August 2015
version: 0.1

Document Revision History

Date	Version Number	Notes
08/19/2015	0.1	Official Release

Acknowledgements: The research project motivating development of the compuGUT was funded in part by an Ontario Ministry of Agriculture, Food and Rural Affairs (OMAFRA) grant. Additionally, the authors would like to show their gratitude to Drs. Emma Allen-Vercoe, Steve Brooks, and Martin Kalmokoff for their valuable consultation and commentary.

Disclaimer: The compuGUT is a research and experimentation tool intended to provide academic and industrial researchers an *in silico* platform to explore ideas governing mechanistic relationships between intestinal physiology, diet and microbiota composition. The authors, however, cannot guarantee the accuracy of results generated from modified versions of the compuGUT source code, and cannot validate clams of others based on results generated using the compugGUT. We encourage user to communicate known issues with the source code and validate their findings with additional simulation, clinical or experimental trials.

The compuGUT makes use of external libraries (SUNDIALS, googleVis). The providers of these libraries do not promote or have any affiliation with the compuGUT software tool or generated results.

Contributors:

Current Contributors: Arun S. Moorthy
e: amoorthy@uoguelph.ca

Hermann J. Eberl
e: heberl@uoguelph.ca
t: 1-519-824-4120 x 52622

Biophysics Interdepartmental Group &
Department of Mathematics and Statistics
University of Guelph, Guelph, Ontario, Canada

Past Contributors: Kathleen Songin (Summer 2014)
Richard Yam (Summer 2014)
Jesse Knight (Summer 2013)

Availability and requirements:

Project Name: compuGUT
Project homepage: http://compugut.sourceforge.net
Operating system(s): Linux
Programming Language: C, R
Other requirements: R, googleVis API and flash enabled browser
License: GNU GPL v3
Any restrictions to use by non-academics: no

Contents

1 Introduction

The large intestine, or colon, is the terminal portion of the human gastro-intestinal tract (GIT). Its primary functions are nutrient absorption and waste preparation. The colon is also host to upwards of 400 species of microorganisms which bring a variety of additional functionality. Unfortunately, the colon is difficult to investigate due to its physical inaccessibility and so, what would seem like routine experimentation is infeasible. Provided as Appendix A (and briefly in Section 1.1), we constructed a mathematical model of carbohydrate digestion and transport processes (exchange and convection) in the human large intestine, extending the model of [19] to consider a spatially continuous physical representation and increased microbial complexity. The resulting model is a system of first order partial differential equations (PDEs) with a user-specifiable number of dependent variables, and stiff, non-linear source terms. Due to the variability in problem size, numerical integration of the mathematical model poses certain organizational challenges. Furthermore, the size of the resulting datasets itself provides both analytical and visualization challenges. As such, we present the *compuGUT* simulation platform as a means to organize and implement our model of biophysical processes in the colon - a platform that can be used as a complimentary tool in investigating microflora in the human large intestine.

1.1 Model Formulation

To the best of our knowledge, the mathematical model of carbohydrate degradation presented in [19], herein referred to as the MT model, is the most complete model of anaerobic digestion in physical environments mimicing the colon. The MT model builds upon the Anaerobic Digestion Model No. 1 (ADM1) [2] framework for describing biochemical and physico-chemical processes involved in anaerobic digestion. The MT model assumes carbohydrates to be the sole substrate entering the colon (disregarding proteins, lipids, and subsequent metabolites), and that distinguishing microbes by their functional involvement as biomass functional groups (BFGs) rather than traditional biological taxa is sufficient in capturing the effective capabilities of the microbial communities, resulting in the digestion processes being described in 17-state variables (sugar, lactate, acetate, proprionate, butyrate, dissolved hydrogen, hydrogen gas, dissolved methane, methane gas, dissolved carbondioxide, carbondioxide gas, polysaccharide, sugar utilizing biomass, lactate utilizing biomass, acetogens, methanogens)[19]. Additionally, the MT model attempts to capture the physical structure of the colon in a manner similar to a 3-stage reactor *in vitro* system with porous polysaccharide matrix to immobilize microbial cultures, distinguishing three physical locations (proximal, transverse, distal colon) and two biochemical environments (lumen and mucus) - leading to a final system of 102-ODEs describing anaerobic digestion in the colon.

Following our work assessing the effect of physical reactor representations in the MT model, we concluded that further investigation of reactor representation on the effect of microflora composition was required [16]. Subsequently, we have developed a spatially continuous framework for modeling processes in the human large intestine; analogous to a continuous pipe plug flow reactor (PFR) with a fluid medium transporting through the pipe, and a fixed-medium of constant volume attached to pipes inner surfaces.

As previously noted, there are reports of the colon being host to as many as 400 different species of microbes. And though many of these species may be redundant in function, the abundance and composition of this intestinal community has been suggested as an important contributor to health (See [3] and references there in). In [22], the authors extend the ADM1 model framework to simulate *species* of microbes within a biomass functional group. In particular, each biomass functional group within the ADM1 model was subdivided into 10 representatives where species can be identified within a group based on their specified biochemical reaction parameters. We adapt a similar idea to extend the MT model of digestion in the colon to consider multiple strains as well. Herein, we refer to this extended model as the *e*MT model.

Combining the previously described PFR-type reactor representation and the *e*MT model of carbohy-

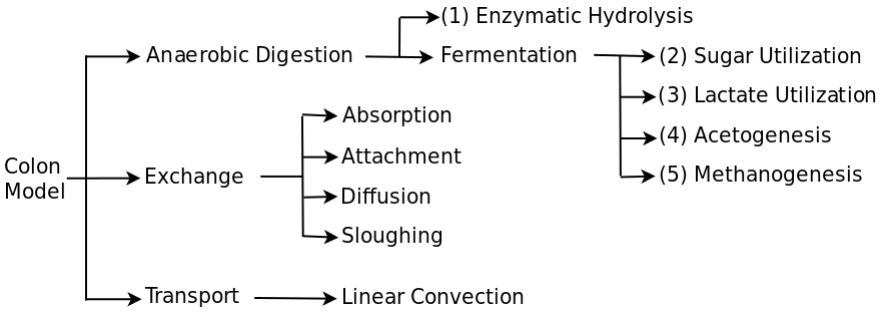

Figure 1: Schematic overview of compuGUTs underlying mathematical models. 5-step model of anaerobic digestion adapted from [19] with modifications to yield parameters ensuring mass conservation in compuGUT implementation.

drate digestion, we have created a spatially continuous mathematical model of transport processes, anaerobic digestion, and microbial complexity as would be expected in the large intestine. The resulting model is a system of first-order PDEs with an unfixed number of dependent variables and stiff, non-linear source terms - a model that cannot be quantitatively assessed with analytical rigour or validated using any existing experimental systems/models, but lends itself naturally to computational implementation and numerical simulation. A schematic representation of biophysical processes considered in the mathematical model is presented as Figure 1.

2 Implementation

The compuGUT suite of tools was developed for Linux systems, and performs three primary tasks: (1) Simulation Design, (2) Numerical Integration, and (3) Data Visualization. Tasks (1) and (3) are performed by auxiliary tools written as either BASH or R scripts, while task (2) is performed by our primary compuGUT tool, written in C. The general work flow is summarized in Figure 2. The compuGUT requires traditional c-libraries (stdlib, stdio, math, string, time, errno) as well as external libraries, namely, the sundials package for solving non-linear problems [10]. The compuGUT interactive visualization tools make use of the googleVis API [6]. As of now, the compuGUT has been tested on 32 and 64-bit Linux workstations.

2.1 Basic Simulation Design Options

Basic simulation parameters in the compuGUT tool are those that can be adjusted by making modifications to input text files. These changes can thus be made without needing to modify and subsequently re-compile the numerical integration source code, and can be automated using scripts. Basic design parameter files are summarized as follows:

A - Operations: Provides options for model sizing, including the physical colon representation (length, radius, etc.) as well as mathematical variables (average system flow rate, biomass representation, 3-stage reactor system versus spatially continuous), as well as general simulation options, such parameter variance for stochastic simulations, number of grid points for numerical discretization, and data output frequency.

B - Diet: Defines the amount of fiber [g] consumed every hour for up to a maximum of 168 hours (7 days).

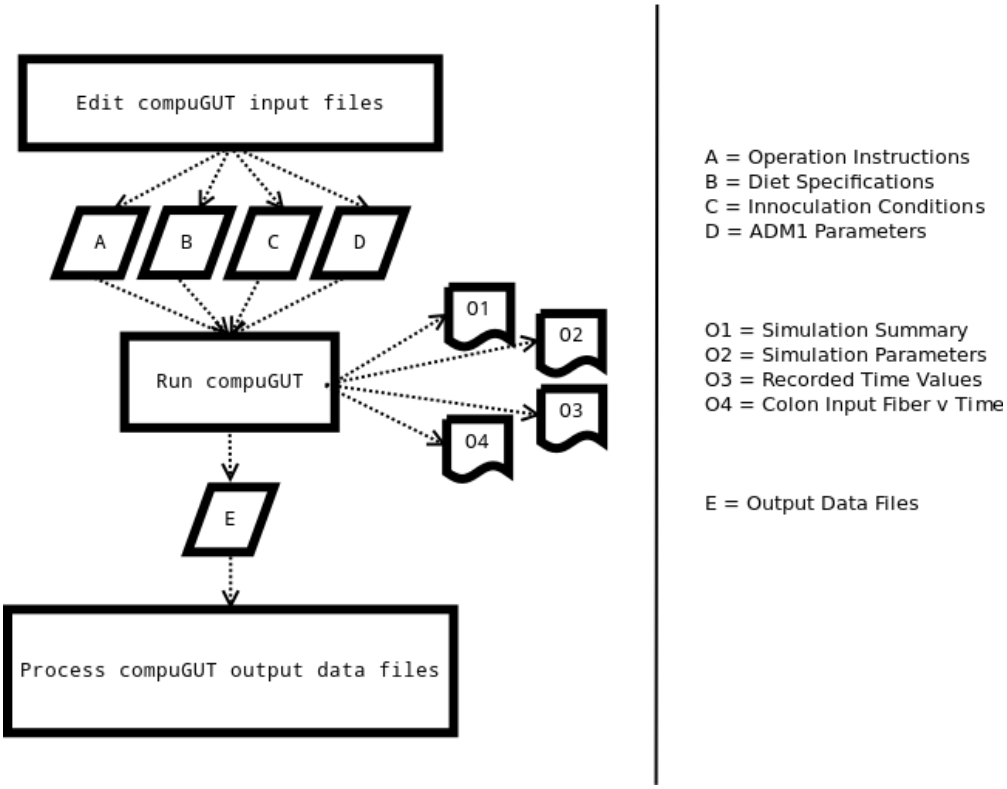

Figure 2: Schematic representation of compuGUT flow of operations. Files A, B, C and D are input files and O1, O2, O3, and O4 are output summary files. The primary integration module is written in C programming language. Additional tools for editing input files and visualizing output files are prepared as R scripts.

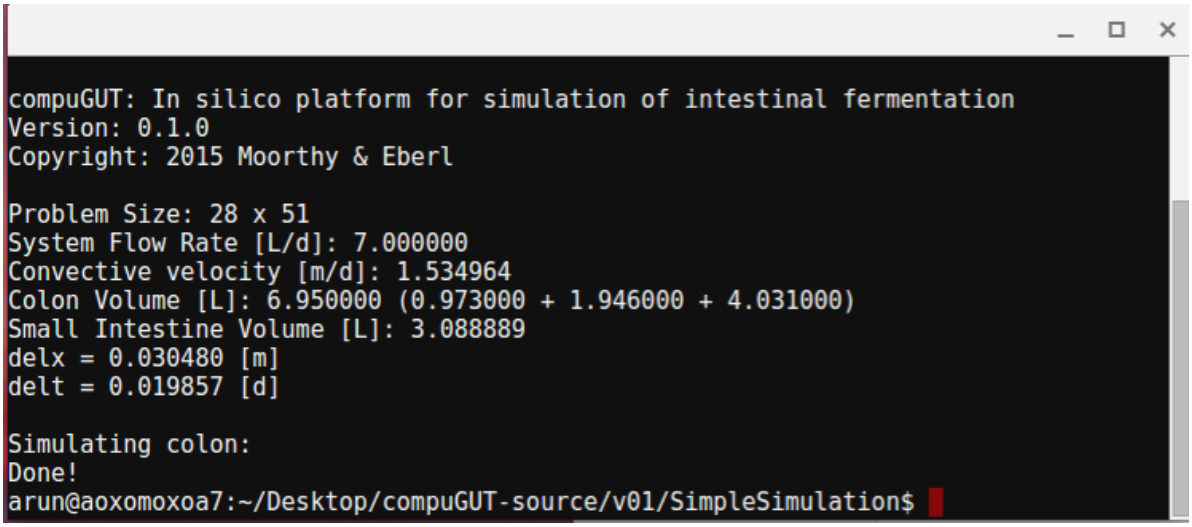

Figure 3: Screen capture of a compuGUT simulation executed in a Linux terminal.

C - Innocula (initial conditions): Prescribes the initial concentration [g/L] of biomass per functional group in the mucus environment. If there are multiple strains/species within a functional group, the concentration is split evenly amongst strains.

D - Reaction Parameters: Sets biochemical reaction parameters (yield coefficients, kinetic rates, half-saturation constants/concentrations) as well as exchange parameters for discrete colon locations (proximal, transverse, and distal).

These basic parameter files are contained within the 'InputFiles' folder and are called upon during numerical simulation.

2.2 Advanced Simulation Options

Advanced simulation parameters require the user to make modifications directly to the C source code. Subsequently, this requires that user re-compile for changes to take effect prior to commencing simulation experiments. Advanced parameters include:

- length of meal
- spline parameters (proximal-transverse and transverse-distal transition location, transition size)
- non-linear solver (SUNDIALS) tolerances

These parameters are embedded within the source code to avoid changes leading to volatile behaviour, particularly with respect to the solver tolerances.

2.3 Numerical Integration

The most involved component of the compuGUT suite is the numerical integration of our defined system of PDEs. Though the model takes a structure similar to many transport models with reactions seen in Engineering application, the combination of both non-linear reaction terms and linear exchange terms between a fluid and stationary medium creates individual sub-processes proceeding at different time scales. This manifests as significant stiffness in the modelled source terms. As such, we employ a central scheme for balance laws [12] to numerically integrate our model system.

This implicit numerical scheme requires the solution to a number of non-linear problems. Rather than employ our own non-linear solvers, we turn to the SUite of Nonlinear and DIfferential/ALgebraic equation Solvers (SUNDIALS) library made available by Lawrence Livermore National Laboratory [10]. The output of the numerical solver is a dataset composed of text files containing the concentration of every dependent variable at every length along the colon for every n number of iterations as defined in the user-operation input file. For a 28 day simulation of a colon with 51 location grid points and standard flow rate of 7 L/d (giving a mean-transit time of approx. 1 day), this results in a data set of 1411 text files. In addition to data, 4 simulation summary text files are generated:

SimulationParameters.txt - biochemical reactiona and exchange parameters used (as these vary during stochastic simulations)

TimeValues.txt - time value for every output data sheet

PreColonData.txt - colon input (output from blackbox pre-gut treatment)

SimulationSummary.txt - overall summary of simulation details (see 4).

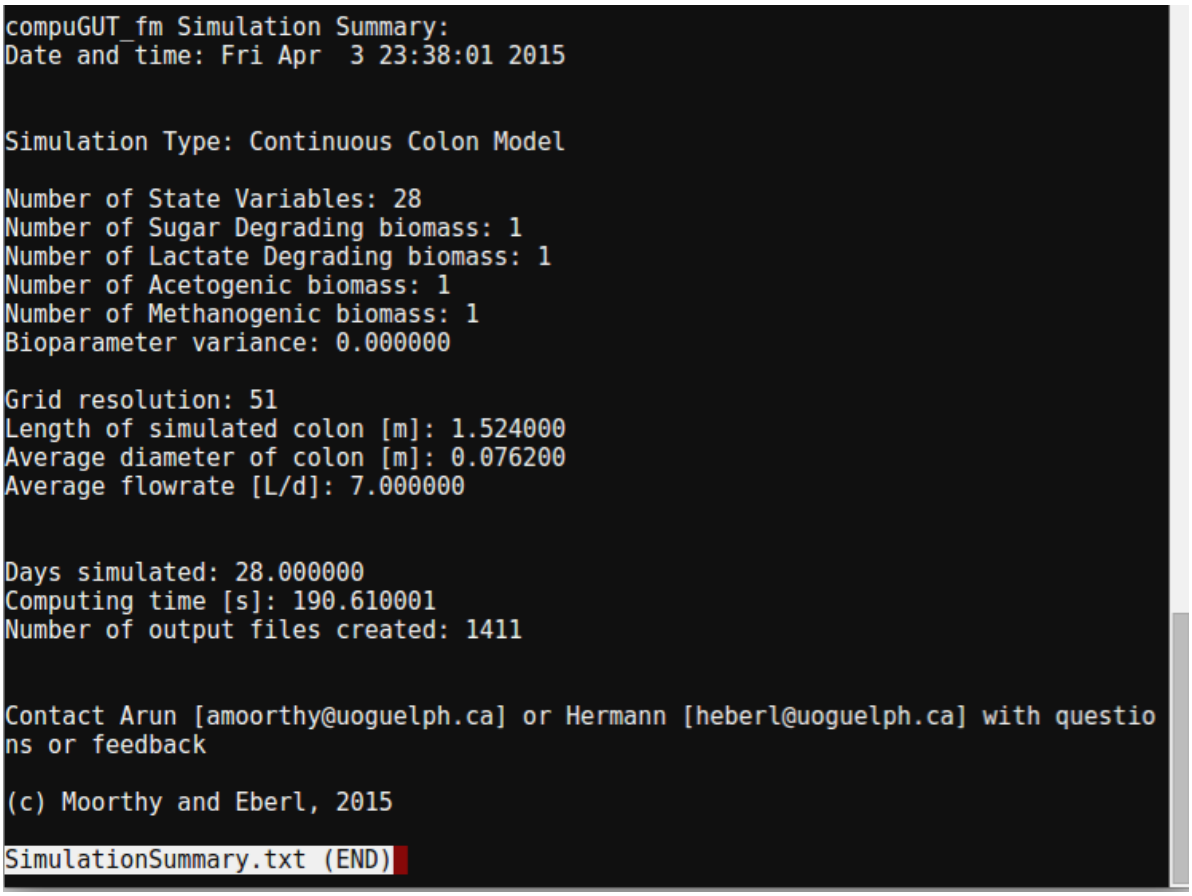

Figure 4: Screen capture of 'SimulationSummary.txt' summary output file for standard 28 day simulation with singular representation in biomass functional groups and a spatial discretization of 51 grid points.

2.4 Data Analysis and Visulization

The second most involved aspect of the compuGUT is data analysis and visualization. As noted, simulations generate high dimensional data. We have included a few elementary plotting and analysis scripts that generate specific types of figures (composition at a colon location at a particular time), as well as a more advanced R markdown document that incorporates the googleVis API to create html objects, allowing users to interact with the data through a flash-enabled browser.

3 Compilation Instructions

The compuGUT platform for in silico simulation of intestinal fermentation is an open source tool written in C. Compilation of the source (access to advanced options) requires libraries developed by the Lawrence Livermore National Library (SUNDIALS), specifically the non-linear solver (KINSOL) and ODE solver (CVODES). Binaries generated in 64-bit Linux using intel and gnu compilers, and 32-bit linux using the gnu compiler are also provided and may be suitable for some users.

Dependencies:

- cvODE-2.7.0
- KINSOL-2.7.0

  Available at: http://computation.llnl.gov/casc/sundials/main.html

BUILDING FROM SOURCE (Linux Instructions):

1. Download compressed folder of latest compugGUT version from project url: compugut.sourceforge.net
2. Navigate to the download location and uncompress compuGUT

   ```
   \$ tar -xf compugGUT-v01.tar
   ```

3. Navigate to uncompressed folder.

   ```
   \$ cd compuGUT-v01
   ```

4. Change permissions of 'quick-compile-X.sh' script to executable, where X is either 32 or 64 depending on your system.

   ```
   \$ chmod 744 quick-compile-X.sh
   ```

5. Run quick-compile-X.sh script to generate compuGUTv01-lXg binary, where X is either 32 or 64, and 'l' and 'g' indicate that the binary is functional on linux operating systems and was compiled using a gnu compiler (gcc).

   ```
   \$ ./quick-compile-X.sh
   ```

EXECUTING BINARY (Linux Instructions):
Users can also use the pre-compiled binary if relevant.

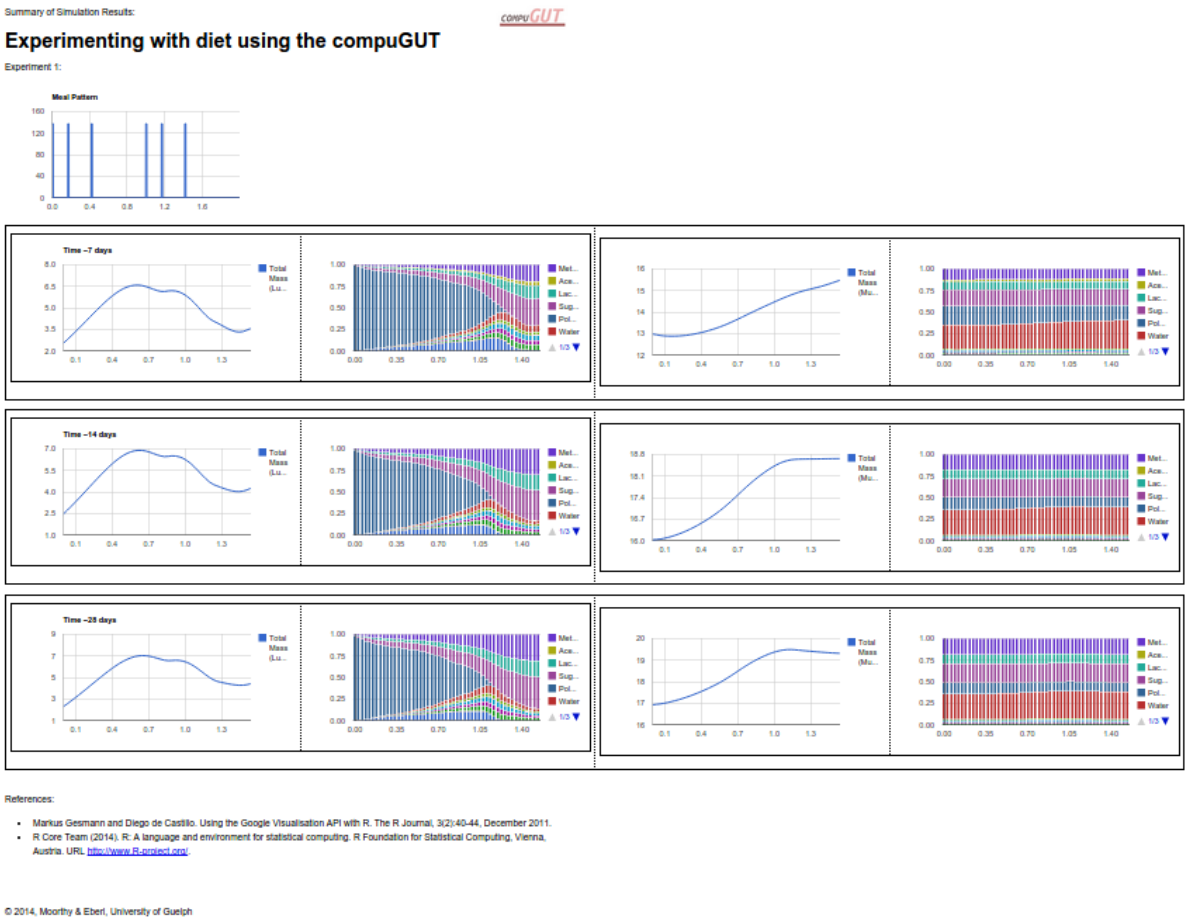

Figure 5: Screen capture of interactive plot results from compuGUT simulation with repeated regular diet. Web-based plots are used for preliminary data-interaction. Figures are best viewed through electronic display, with full results available at compuGUT project webpage: http://compugut.sourceforge.net

```
\$ ./compuGUTv01-l64g
```

INTERACTIVE R-Scripts:
R-scripts are require significant user modification. Additional packages are required as noted in the scripts themselves.

4 Usage Examples

4.1 Regular Diet Simulation

We define a 'regular' dietary regime as one that is both periodic in terms of meal frequency and constant in terms of meal amount. For example, Figure 5 is a screen capture of a compuGUT output html for a simulation with regular diet; 10 grams of fiber per meal and meals are consumed at hours 0, 4 and 10 (e.g. 8am, 12pm, 6pm) every day for 28 days. We note that with that this type of regularity, the composition of material along the colon has inconsequential changes in either the lumen or mucus environment as a function of time once transient effects due to initial/innoculation conditions are accounted for.

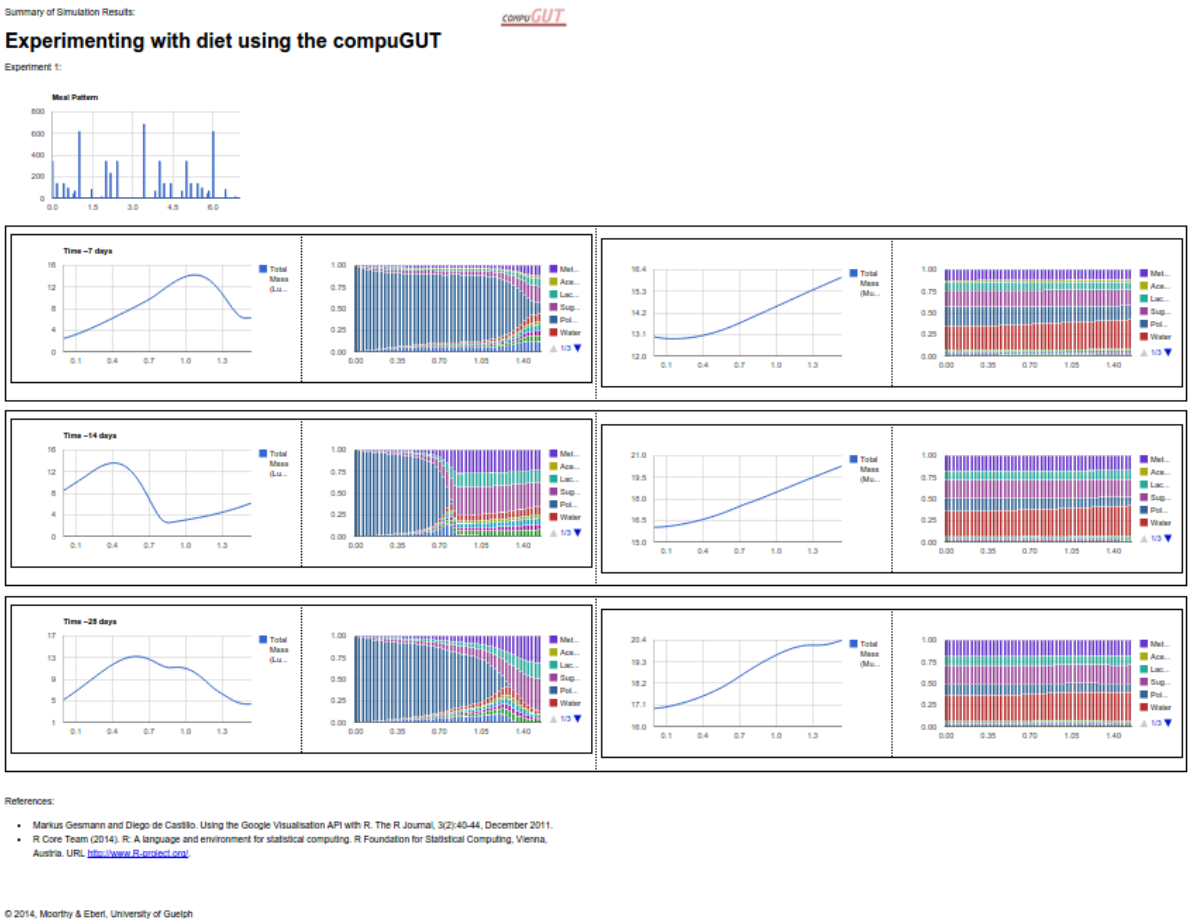

Figure 6: Screen capture of interactive plot results from compuGUT simulation with repeated irregular diet. Web-based plots are used for preliminary data-interaction. Figures are best viewed through electronic display, with full results available at compuGUT project webpage: http://compugut.sourceforge.net

4.2 Irregular Diet

We define an 'irregular' dietary regime as one that is either irregular in terms of meal frequency and/or meal amount. For example, Figure 6 is a screen capture of a compuGUT output html for a simulation with irregular diet, highlighted in the top left of the figure where the dietary fiber intake in the first 7 days of simulation is provided. In the case of our simulation, this 7 day pattern is then repeated 3 more times to fulfill our 28 day simulation. We note that these irregularities do infact have substantial effects on the material composition along the colon as a function of time, but not nearly as noticable effect in the mucus environment.

4.3 Simulation Experiment

To fully utilize the power of the compuGUT, we highlight results of a simulation experiment; a sequence of simulations used to validate or invalidate an idea, theory or claim. Here we investigate how the colon microflora composition varies as a result of three factors: (1) the total amount of fiber consumed, (2) the number of meals in which the fiber is distributed, and (3) the length/intensity of the meal. We assess these factors by testing 18 scenarios highlighted in Figure 7. As a demonstrative simulation experiment, we draw

Summary of Simulation Results:

compuGUT

Experimenting with diet using the compuGUT

Purpose:

In this study, we assess the effect of 3 dietary components as available in the compuGUT simulation tool. These 3 components include:

- (1) Fiber per day (low - 15, average - 30, high - 45)
- (2) Number of meals / Feeding Pattern (3, 5, or 10 meals per day)
- (3) Length of meal (15 minutes or 30 minutes)

Method:

We define 3-factors of 3, 3 and 2 levels. Thus, to assess all levels of all factors, we require 3 x 3 x 2 experiments (18). The parameters of these experiments is as follows:

Exp #	No. of Meals	Total Fiber per Meal [g]	Fiber per Day [g]	Length of Meal [h]	Mean Transit Time [d]
1	3	5	15	0.25	1
2	3	10	30	0.25	1
3	3	15	45	0.25	1
4	3	5	15	0.5	1
5	3	10	30	0.5	1
6	3	15	45	0.5	1
7	5	3	15	0.25	1
8	5	6	30	0.25	1
9	5	9	45	0.25	1
10	5	3	15	0.5	1
11	5	6	30	0.5	1
12	5	9	45	0.5	1
13	10	1.5	15	0.25	1
14	10	3	30	0.25	1
15	10	4.5	45	0.25	1
16	10	1.5	15	0.5	1
17	10	3	30	0.5	1
18	10	4.5	45	0.5	1

Results:

Experiment 1:

Meal Pattern

References:

- Markus Gesmann and Diego de Castillo. Using the Google Visualisation API with R. The R Journal, 3(2):40-44, December 2011.
- R Core Team (2014). R: A language and environment for statistical computing. R Foundation for Statistical Computing, Vienna, Austria. URL http://www.R-project.org/.

Figure 7: Screen capture of interactive plot results from compuGUT simulation with various regularly repeated diet regimes. Web-based plots are used for preliminary data-interaction. Figures are best viewed through electronic display, with full results available at compuGUT project webpage: http://compugut.sourceforge.net

conclusions by assessing the percent composition of a single biomass functional group at the output (last location) of the colon after 28 days, but note that there is data available for all dependent variable at all locations at multiple timesteps (≈1440) through out the 28 day simulation. From the output assessed, we can conclude that:

- the length of meal (15 minutes versus 30 minutes) has limited effect on the measured output
- the difference between measure output generated through a high-fibre diet and low-fiber diet simulation is amplified when meals are less frequent, and diminished when meals are consumed more frequently

From a fairly simple simulation experiment we were able to draw a substantial conclusion about the importance of meal frequency when assessing the effect of dietary fibre levels.

5 Conclusions

We have a computational tool capable of simulating carbohydrate digestion and transport processes along the length of the human colon; a software implementation of the mathematical model described in [15]. We have discussed some of the current capabilities, including a demonstration of a simple simulation experiment studying meal regiments. However, we note that the underlying mathematical model is built on many assumptions/simplifications and that there are a few potential extensions that are currently in development.

The anaerobic digestion model embedded in the compuGUT is based on the model of carbohydrate digestion developed in [19], and though fibers are the primary source of substrate to intestinal microflora, there have been many examples of the importance of nitrogen and nitrogen sources in the function of intestinal microflora [11]. Adding a source of nitrogen, as well as extending the diversity of fiber-types that can be metabolized using the compuGUT is a priority.

Convective flow in the compuGUT is a very simple first-order convection approximation. This may be extended to capture the dynamic material properties of digesta passing through the colon, evolving from a liquid to semi-solid during the transport process.

Finally, the compuGUT is currently built as a stand-alone tool with no integration techniques with clinical or experimental data. Creating an interface to allow for iterative computational, laboratory and clinical investigation would prove of great value in advancing the mechanistic understanding of intestinal microflora in health and disease.

6 Additional Resources

Users of the compuGUT may find benefit in reviewing the following resources:

1. `http://www.cprogramming.com/`
2. `http://cran.r-project.org/`
3. `http://linuxcommand.org/learning_the_shell.php`

A A spatially continuous model of carbohydrate digestion and transport processes in the colon - Mathematical Details

A.1 Overview

The large intestine is the distal most portion of the gastro-intestinal tract. It is responsible for the final absorption of digestive nutrients and preparation of fecal matter for bowel movements [25]. It is an open tube-like organ with muscular walls to aid in the continued transport of eventual waste materials. The walls of the colon are also lubricated with endogenously produced mucus. The colon is often described in three separate locations: the proximal (or ascending), transverse, and distal (or descending) colon. These three locations have differing physical conditions, specifically with regard to the acidity (with locations closer to the proximal end being more acidic than towards the distal end) and the absorption/transportation rates at which substrates are removed from the colon [25]. The colon's biochemical environment makes it a highly suitable habitat to dense communities of microflora. One of the primary functions of the intestinal microflora is to digest chemically indigestible materials (such as dietary fiber). Metabolites generated through this digestion process are absorbed by the gut, and waste material is transported along the length of the colon. Thus, we can think of colon functionality as being defined by three sub-processes with dynamics governed by the interaction of a complex network of microflora, substrates, metabolites and physical forces, in multiple physically and biochemically diverse environments: (i) the digestion of particulate material, (ii) the exchange of soluble materials between biochemical environments (lumen-mucus-host), and (iii) the convective transport of materials through the length of the colon.

By way of material balance, we can combine the three sub-processes and describe the density of materials in the colon with the following advection-reaction system:

$$\partial_t \mathbf{c} + \partial_x F(\mathbf{c}) = R(\mathbf{c}) + E(\mathbf{c}) \tag{1}$$

where the functions R, F and E can be interpreted as non-linear functions describing the sub-processes of anaerobic digestion, material transport, and component exchange, respectively, and their input, $\mathbf{c}$, is a vector of concentrations [g/L] of all materials considered in the colon-complex. We describe functions R, F and E in detail in the following sections, but present Figure 8 as a schematic representation of the model structure and foundational processes.

A.1.1 Assumptions

Physiological systems are highly complex, functioning with redundancy, time-variations and interplay with other systems [9]. Rather than model the entire physiology of the colon, we look to capture the integral mechanisms defining the colon-diet-flora system with as little complexity as possible. We introduce the following simplifications for model development:

- **Colon Geometry:** A cross-sectional slice of the colon would display highly irregular geometry, as there exists mucousal folds and villous surfaces [8, 23]. For simplicity, the geometry of the large intestine is averaged as a cylindrical tube of constant diameter. Combining this simplification with the knowledge that the length of the colon is significantly larger than its diameter allows us to model the colon as 1-dimensional in space (x-dimension)

- **Material Properties:** To be consistent with our first assumption (1D tube geometry), we assume that the materials in localized portions of the colon (a particular x-value) will be homogeneous (well-mixed) across the cross-sectional area.

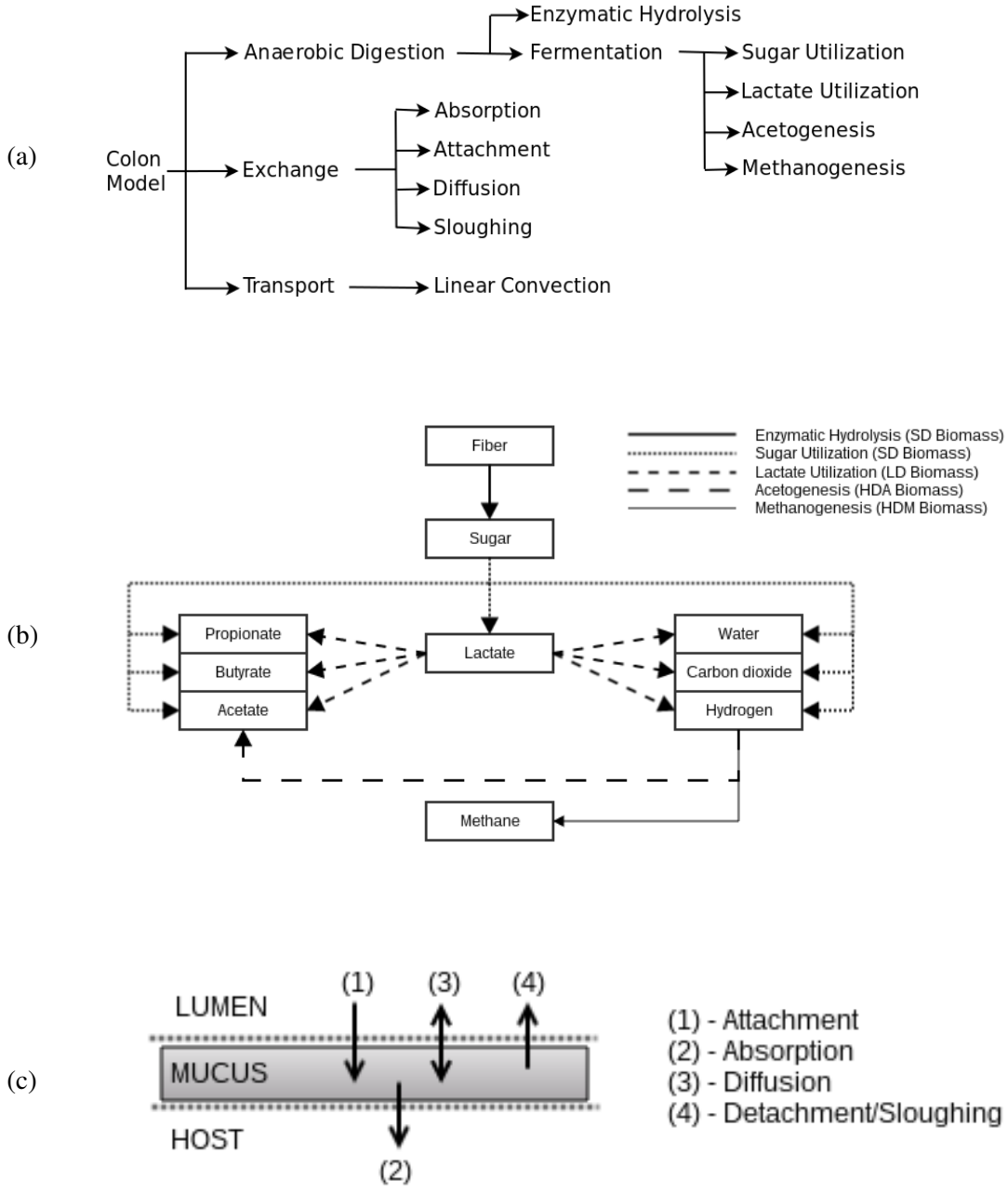

Figure 8: Overview of compuGUTs underlying mathematical model. (a) Schematic overview of biochemical and physical processes considered in the compuGUT. (b) 5-step model of anaerobic digestion, adapted from [19]. Biomass functional group active in each step indicated in parentheses. (c) Summary of component exchange processes. Material in the lumen environment is transported along the length of the colon where as mucus material is stationary along the length of the colon and only experiences axial transport.

- **Mucus Thickness:** Mucus is produced endogenously through out the colon. The rate of this mucus production is constant in all locations. Additionally, we treat this layer as a fixed medium of constant volume, with the volume of the mucus being 10% of the total colon volume.

- **Transit Time:** The effect of peristalsis and additional propulsion mechanisms manifest as an average flow or speed of convective transport. This allows us to approximate convective transport as a first-order flux with constant velocity term.

- **Metabolic Pathways:** The only macromolecules reaching the colon are carbohydrates, and the anaerobic digestion of carbohydrates follows the metabolic pathway described in [19]. This metabolic pathway can be summarized as a five-step process (highlighted in Figure 8b), where fiber is first hydrolyzed to monomer sugars, and then monomer sugars are fermented by intestinal microflora into various metabolites (lactate, acetate, propionate, butyrate, hydrogen, methane, carbon dioxide, and water) in the parallel processes of sugar utilization, lactate utilization, acetogenesis and methanogenesis. Though there are over 400 species of microbes inhabiting the colon [4], we assume that the total flora in the colon can be sub-divided into four biomass functional groups according by fermentation step. Thus we define flora as either Sugar Fermenters (SD), Lactate Fermenters (LD), Hydrogen Oxidizing Acetogens (HDA), or Hydrogen Oxidizing Methanogens (HDM). Hydrolysis progresses due to enzymes produced by SD flora. These assumptions are adapted directly from the works of [1, 2, 19], and is a familiar approach in most lines of microbial modeling and engineering.

- **Reaction Processes:** Combining the processes involved in metabolism and the natural decay of flora in the system, we can summarize the reaction processes in the flora-diet system as: (1) hydrolysis, (2) glucose utilization, (3) lactate utilization, (4) acetogenesis, (5) methanogenesis, (6) decay of SD flora, (7) decay of LD flora, (8) decay of HDA flora, and (9) decay of HDM flora. The choice of metabolic pathways and subsequent reaction processes is responsible for the overall model problem size, thus a simpler representation of anaerobic digestion would lead to a smaller state-space, and a more involved representation of anaerobic digestion would lead to a larger state space.

We remark that the model assumptions and simplifications can be relaxed on future model iterations as knowledge of functional details continues to grow, but doing so would require the inclusion of additional mathematical and numerical complexities.

A.1.2 Notation

For organizational convenience, we introduce notation conventions prior to proceeding with the model construction. With the size, complexity and included variability of the mathematical description, the model is more naturally suited for numerical investigation. Accordingly, we follow a computational array/indexing organization scheme, which will also allow for discussion of the software implementation.

Indices Our primary indices are i, j, and e. Index i indicates particularity within a solution array/parameter grouping. Index j indicates particularity within index i (if needed). Index e, when associated with a model variable or parameter indicate the biochemical environment (lumen or mucus) in which that particular component exists or parameter is used. Index e takes the value 1 if describing a lumen variable, and 2 if identifying a mucus variable. Descriptions of the solution arrays and parameter groupings in which these indices are used is to follow, and will aid in clarity.

Dependent variables We notate our comprehensive solution array (all dependent variables) by the vector $\mathbf{c}$ - concentration, where $\mathbf{c} = [\mathbf{S}, \mathbf{I}, \mathbf{X}]^T$, and the components of sub-solution arrays $\mathbf{S}$ - soluble substrates/metabolites/compounds, $\mathbf{I}$ - insoluble carbohydrates, and $\mathbf{X}$ - biomass, are defined as follows:

$$S_{e,i_s} \quad \text{where} \quad i_s \in [1,2,3,4,5,6,7,8,9], \tag{2}$$

$$I_{e,i_i} \quad \text{where} \quad i_i \in [1], \tag{3}$$

$$X_{e,i_x,j_{i_x}} \quad \text{where} \quad i_x \in [1,2,3,4], \quad j_{i_x} \in [1,2,...,n_{i_x}], \tag{4}$$

and index $e \in [1,2]$ is as previously defined. All dependent variables are concentrations measured in [g/L]. The use of subscripts with indices i and j is to make clear that their values are dependent on the solution array ($\mathbf{S}, \mathbf{I}, \mathbf{X}$) or biomass functional group (in the case of j) being considered. Moving forward, we drop these subscripts for legibility whenever possible but do include them in situations which may otherwise read ambiguously. The use of index j when describing biomass quantities is to identify *a strain or species* within the biomass functional group indexed by i, where the maximum value of j is n_i. That is, $X_{2,3,5}$ would identify the concentration of the 5th *species* of acetogenic biomass ($i = 3$) in the mucus environment ($e = 2$). Details on how strains are defined are to follow in Section A.2.1. A summary list of dependent variables, including their mathematical identification and numerical implementation indices is given in Table 1. Referring back to the overall solution array $\mathbf{c}$, we can summarize the overall problem (system) size as:

$$\dim(\mathbf{c}) = \max(e) \times \left(\max(i_s) + \max(i_i) + \sum_{i=1}^{\max(i_x)} \max(j_i) \right), \tag{5}$$

detailing that the problem size is equal to the sum of the maximum number of substrate, fiber, and biomass representations multiplied by the number of environments (lumen and mucus). For the most simple model scenario we present (1 strain per biomass functional group), this would mean a state vector of 28 elements (9 substrates, 1 fiber, 4 biomass functional groups, 1 strain per biomass functional group, 2 environments), and for the most complex scenario that we have tested, a state vector of 100 elements (9 substrates, 1 fiber, 4 biomass functional groups, 10 strain per biomass functional group, 2 environments).

Parameters The model contains many parameters of similar definition, so standardized notation is used to maintain organization.

There are four primary groups of parameters: yield coefficients (Y), kinetic rates (κ), half-saturation constants and concentrations (K), and exchange rates (γ). Additional physical (lengths, volumes, etc.) and operational (variance, spline constants) parameters exist, but will be described as they are introduced in the text.

Yield coefficients describe the affects of anaerobic reaction process on the density of system variable. We use the following standard notation:

$$Y_{i_c,p_r,j_{i_x}} \quad \text{where} \quad p_r \in [1,2,3,4,5,6,7,8,9], \quad j_{i_x} \in [1,2,...,n_{i_x}] \tag{6}$$

indicating the yield of system variable i_c consumed or generated in the anaerobic reaction process (see Section 1.1) p_r performed by strain j_{i_x} of biomass functional group i_x. It should be noted that yield coefficients exist for all components of vector $\mathbf{c}$, hence the use of index i_c. That said, not all components are involved in all processes, leading to yield coefficients of zero.

Table 1: Summary of dependent variable notation used to describe the colon-complex. C.Index indicates the index value used in numerical implementation, whereas indices i, j and e indicate index values used for mathematical development, as described in Section A.1.2.

C.Index	Solution Array	i	j	e	Component
1	S	1		1	Lumen glucose
2		1		2	Mucus glucose
3		2		1	Lumen lactate
4		2		2	Mucus lactate
5		3		1	Lumen hydrogen
6		3		2	Mucus hydrogen
7		4		1	Lumen acetate
8		4		2	Mucus acetate
9		5		1	Lumen propionate
10		5		2	Mucus propionate
11		6		1	Lumen butyrate
12		6		2	Mucus butyrate
13		7		1	Lumen methane
14		7		2	Mucus methane
15		8		1	Lumen carbon dioxide
16		8		2	Mucus carbon dioxide
17		9		1	Lumen water
18		9		2	Mucus water
19	I	1		1	Lumen polysaccharide (fiber)
20		1		2	Mucus polysaccaride (mucin)
$2(10)+1$	X	1	1	1	Lumen sugar utilizing biomass - strain 1
$\vdots$					
$2(10+n_1)$		1	n_1	2	Mucus sugar utilizing biomass - strain n_1
$2(10+n_1)+1$		2	1	1	Lumen lactate utilizing biomass - strain 1
$\vdots$					
$2(10+n_1+n_2)$		2	n_2	2	Mucus lactate utilizing biomass - strain n_2
$2(10+n_1+n_2)+1$		3	1	1	Lumen acetogenic biomass - strain 1
$\vdots$					
$2(10+\sum_i^3 n_i)$		3	n_3	2	Mucus acetogenic biomass - strain n_3
$2(10+\sum_i^3 n_i)+1$		4	1	1	Lumen methanogenic biomass - strain 1
$\vdots$					
$2(10+\sum_i^4 n_i)$		4	n_4	2	Mucus methanogenic biomass - strain n_4

Kinetic parameters specify the maximum rate at which a reaction process indexed by p_r and governed by biomass strain j_{i_x} proceeds, and takes the standard notation:

$$\kappa_{p_r,j_{i_x}} \quad \text{where} \quad p_r \in [1,2,3,4,5,6,7,8,9], \\ j_{i_x} \in [1,2,...,n_{i_x}]. \tag{7}$$

Similarly, many of our considered reaction kinetics have half saturation constants or concentrations, following the standard notation:

$$K_{p_r,j_{i_x}} \quad \text{where} \quad p_r \in [1,2,3,4,5,6,7,8,9], \\ j_{i_x} \in [1,2,...,n_{i_x}]. \tag{8}$$

Lastly, specific rates are used to describe the way material is exchanged between biochemical environments using 4 exchange mechanisms indexed by p_e, taking the standard notation:

$$\gamma_{i_c,p_e} \quad \text{where} \quad p_e \in [1,2,3,4]. \tag{9}$$

Like yield coefficients, exchange rates exists for all components of the solution array $\boldsymbol{c}$ for each exchange process, which is why we use the index i_c. A complete list of all biochemical reaction (Yield and rate coefficients) and exchange parameters with default values is provided in Tables 2 and 3, and all physical and operation parameters are defined in Tables 4 and 5.

A.2 Model Development

We construct the mathematical model using material balances to describe how quantities in the colon-complex change with time and space. The result is a system of partial differential equations with functional representations of sub-processes as summarized in (1).

A.2.1 Anaerobic Digestion

As noted in our primary assumptions, the choice of anaerobic digestion/metabolic pathway is key to determining the size and structure of the mathematical model. Digestion occurs throughout the length of the colon, and in both the lumen and mucus environments. For clarity, we describe our model of anaerobic digestion independent of location and environment.

MT-Model A model of anaerobic digestion specific to the environmental conditions of the human colon was developed in [19], simplifying the Anaerobic Digestion Model No. 1 (ADM1) system described in [2] to only consider carbohydrate particulate waste (as opposed to including proteins and lipids as well), and employ lumen and mucus *environments* to describe the colons physical structure. We refer to this model as the MT-model of carbohydrate digestion. The resulting model describes anaerobic digestion in two processes (enzymatic hydrolysis and fermentation) consisting of five metabolic steps, all of which are driven by the presence of microflora, and the natural decay of biomaterial from the system.

> **Enzymatic Hydrolysis:** Enzymatic hydrolysis is the degradation of polysaccharides into simple monosaccharides in the presence of enzymes produced by sugar utilizing biomass. The complete process of enzymatic hydrolysis is quite complex and is composed of a large number of intermediate steps [7, 27]; however, mathematical models of the rate of hydrolysis are often simplified to statements of first-order based on observation and empirical data [5]. In [19], the authors suggest modeling hydrolysis by *Contois* kinetics, as equations of this form are well adapted for modeling a wide range of substrate-biomass scenarios [26]. As such, we model the rate of hydrolysis (ϕ_1) as follows:
>
> $$\phi_1 = \frac{\kappa_1 I X_1}{I + K_1 X_1}, \tag{10}$$

Table 2: List of default simulation biochemical reaction parameters. **YC**: Yield Coefficient, **SR**: Specific Rate **CR**: Concentration Ratio, **HS**: Half-Saturation. Column one presents the parameter reference number used in the sensitivity analysis. Yield coefficients are derived using stoichiometry balances (Section A.2.1). Reaction parameter values adapted from [19]. Yield parameters are described in grams of product per gram of limiting reactant for ease of identification.

SA ref.	Symbol	Parameter	Value
	$Y_{1,1}$	YC sugar from fiber	1 g_{su}/g_z
	$Y_{2,2}$	YC lactate from sugar	0.0901 g_{la}/g_{su}
	$Y_{3,2}$	YC hydrogen from sugar	0.00606 g_{H_2}/g_{su}
	$Y_{4,2}$	YC acetate from sugar	0.12121 g_{ac}/g_{su}
	$Y_{5,2}$	YC propionate from sugar	0.14949 g_{pro}/g_{su}
	$Y_{6,2}$	YC butyrate from sugar	0.04444g_{but}/g_{su}
	$Y_{3,3}$	YC hydrogen from lactate	0.00444 g_{H_2}/g_{la}
	$Y_{4,3}$	YC acetate from lactate	0.06667 g_{ac}/g_{la}
	$Y_{5,3}$	YC propionate from lactate	0.16444 g_{pro}/g_{la}
	$Y_{6,3}$	YC butyrate from lactate	0.09778 g_{but}/g_{la}
	$Y_{4,4}$	YC acetate from hydrogen	2.14286 g_{ac}/g_{H_2}
	$Y_{7,5}$	YC methane from hydrogen	0.57143 g_{CH_4}/g_{H_2}
	$Y_{8,2}$	YC carbon dioxide from sugar	0.13333 g_{CO_2}/g_{su}
	$Y_{8,3}$	YC carbon dioxide from lactate	0.14667 g_{CO_2}/g_{la}
	$Y_{8,4}$	YC carbon dioxide from hydrogen (acetogenesis)	-11.000 g_{CO_2}/g_{H_2a}
	$Y_{8,5}$	YC carbon dioxide from hydrogen (methanogenesis)	-9.42857 g_{CO_2}/g_{H_2}
	$Y_{9,2}$	YC aqueous water from sugar	0.12364 g_{H_2O}/g_{su}
	$Y_{9,3}$	YC aqueous water from lactate	0.20000 g_{H_2O}/g_{la}
	$Y_{9,4}$	YC aqueous water from hydrogen (acetogenesis)	6.42857 g_{H_2O}/g_{H_2a}
	$Y_{9,5}$	YC aqueous water from hydrogen (methanogenesis)	6.42857 g_{H_2O}/g_{H_2m}
	$Y_{11,2}$	YC sugar degrading bacteria	0.3424 $g_{X_{su}}/g_{su}$
	$Y_{12,3}$	YC lactate degrading bacteria	0.37667 $g_{X_{la}}/g_{la}$
	$Y_{13,4}$	YC acetogenic bacteria	4.035714 $g_{X_{H_2a}}/g_{H_2}$
	$Y_{14,5}$	YC methanogenic bacteria	4.035714 $g_{X_{H_2m}}/g_{H_2}$
1	κ_1	SR hydrolysis	10.6195 $g_z/g_{X_{su}} \cdot d$
2	κ_2	SR sugar consumption	12.6271 $g_{su}/g_{X_{su}} \cdot d$
3	κ_3	SR lactate consumption	82.1083 $g_{la}/g_{X_{la}} \cdot d$
4	κ_4	SR hydrogen consumption by acetogenic bacteria	1.9263 $g_{H_2}/g_{X_{H_2a}} \cdot d$
5	κ_5	SR hydrogen consumption by methanogenic bacteria	0.3997 $g_{H_2}/g_{X_{H_2m}} \cdot d$
6	K_1	CR (hydrolysis)	0.2654 $g_z/g_{X_{su}}$
7	K_2	HS concentration sugar	0.4684 g_{su}/L
8	K_3	HS concentration lactate	0.5969 g_{la}/L
9	K_4	HS concentration hydrogen (acetogenesis)	0.0034 g_{H_2}/L
10	K_5	HS concentration hydrogen (methanogensis)	3.126×10^{-6} g_{H_2}/L
11-14	κ_{6-9}	SR biomass decay	0.01 d^{-1}

Table 3: Matrix of exchange terms for soluble substrates, polysaccharides and biomass concentrations. Functions E_1,E_2,E_3, and E_4 represent transport from lumen to mucus, from mucus to host, between lumen and mucus, and from mucus to lumen, respectively. The *shape* of exchange parameter γ as a function of colon location (Described in Section A.2.2) is shown as a spark figure, with the discrete values in the proximal (P), transverse (T) and distal (D) colon provided in brackets. Exchange parameters are in the units [d^{-1}] except with respect to transport between lumen and mucus (E_3), where the units are [L/d]. Discrete parameter values taken from [19].

Process, p_e		E_1 $[L \rightarrow M]$		E_2 $[M \rightarrow H]$		E_3 $[L \leftrightarrow M]$		E_4 $[L \leftarrow M]$	
Component k		γ_1	[P/T/D]	γ_2	[P/T/D]	γ_3	[P/T/D]	γ_4	[P/T/D]
1	s_s						[1.6/3.8/6.3]		
2	s_l		[0.88/0.43/2.03]		[12.6]				
3	s_h								
4	s_{ac}		[1.32/0.64/3.05]		[18.9]				
5	s_{pr}		[1.07/0.62/2.47]		[15.32]				
6	s_{bu}		[0.9/0.6/2.49]		[12.88]				
7	s_{ch_4}		[1/0.6/3]		[14]				
8	s_{co_2}		[1/0.6/3]		[14]				
9	s_{h_2o}		[1.6/0.77/3.66]		[1.6]				
10	z								[0.1]
11	b_s		[0.1]						[0.4]
12	b_l		[0.1]						[0.4]
13	b_a		[0.1]						[0.4]
14	b_m		[0.1]						[0.4]
Kinetic Rate		$E_1 = \gamma_{1,k} c_{1,k}$		$E_2 = \gamma_{2,k} c_{2,k}$		$E_3 = \frac{\gamma_{3,k}}{V_l}(c_{1,k} - c_{2,k})$		$E_4 = \gamma_{4,k} c_{2,k}$	

Table 4: Physical parameters required for simulation. Parameter values adapted from [19].

Symbol	Parameter	Default Value
L_c	Length of colon [m]	1.524
d_c	Average diameter of the colon [cm]	7.62
L_s	Length of small intestine [m]	6.096
d_s	Average diameter of small intestine [cm]	2.54
V_c	Volume of colon [L]	6.95
V_l	Volume of lumen environment [L]	6.255
V_m	Volume of mucus environment [L]	0.695
$L_{p,t}$	Proximal-Transverse colon length transition percentage	0.14
$L_{t,s}$	Transverse-Distal colon length transition percentage	0.42
q	Average system flow rate [L/d]	7

Table 5: Operation parameters required for simulation. Parameter values adapted from [19].

Symbol		Parameter	Default Value
n_1	(n_{sd})	Number of sugar utilizing biomass representatives	1
n_2	(n_{ld})	Number of lactate utilizing biomass representatives	1
n_3	(n_{hda})	Number of acetogenic biomass representatives	1
n_4	(n_{hdm})	Number of methanogenic biomass representatives	1
σ_b		Variance of biochemical reaction parameters	0.05
σ_p		Variance of exchange parameters	0.0
σ_s		Cubic spline interpolation range (percentage)	0.1
k		Grid Index value	0
N		Number of grid points $((50)2^k + 1)$	51

where variables and parameters are as previously defined.

Fermentation: Fermentation is the process of converting simple sugars to short-chain fatty acids, simple compounds and gases. The steps within fermentation, which occur both sequentially and in parallel, create time sensitivities and model stiffness. Additionally, the rates at which these steps occur is a product of microflora concentration and substrate/metabolite availability. The rates for (i) glucose utilization, (ii) lactate utilization, (iii) acetogenesis, and (iv) methanogenesis, are all modeled using *Monod* kinetics, as:

$$\phi_f = \frac{\kappa S X}{K + S} I_{pH}, \tag{11}$$

where S is the concentration of substrate utilized by biomass X in the completion of a particular fermentation step and I_{pH} is a rate inhibition term due to acidity. Most fermentation steps are not pH inhibited, thus $I_{pH} = 1$.The rate of methanogenesis is inhibited as follows:

$$I_{pH} = \begin{cases} exp(-3\left(\frac{pH - pH_u}{pH_u - pH_l}\right)^2) & \text{if } pH < pH_u, \\ 1 & \text{if } pH \geq pH_u, \end{cases} \tag{12}$$

where pH_u and pH_l are upper and lower pH limits that are dependent on colon location [2, 19].

Natural Decay: The effects of age and damage do apply to microbial systems [24]. This natural decay is included as:

$$\phi_d = \kappa X, \tag{13}$$

where X is a biomass concentration and κ is the specific rate of decay for that particular biomass strain.

Derivation of Yield Coefficients: Each process in the fermentation of simple sugars to SCFAs can be expressed by a balanced chemical equation describing the change from reactants to products. For example, Glucose Fermentation can be described by:

$$\begin{aligned} 11C_6H_{12}O_6 + 6NH_3 \quad \rightarrow \quad & 2CH_3CHOHCOOH + 4CH_3COOH \\ & + 4CH_3CH_2COOH + CH_3CH_2CH_2COOH \\ & + 6H_2 + 6CO_2 + 18H_2O + 6C_5H_7O_2N, \end{aligned}$$

where 11 moles of glucose and 6 moles of ammonia create 2 moles of lactate, 4 moles of acetate, 4 moles of propionate, a mole of butyrate, 6 moles of hydrogen, 6 moles of carbon dioxide, 18 moles of water and 6 moles of biomass, respectively [18]. Biomass involved in glucose utilization is referred to as sugar fermenting or sugar utilizing biomass. The chemical formula for biomass, $C_5H_7O_2N$, is an approximation adapted directly from [2]. Complete chemical balances are provided in Muñoz-Tamayo et. al [19]. For ease of analysis, Tables 6-9 are presented in place of chemical formula to describe the complete reactions associated with fermentation.

Yield coefficients for each product in each reaction process are derived using the mass basis of the process limiting reactant. Process limiting reactants are identified using boldface in each of the respective tables. For example, the yield of propionate (product) from lactate (reactant) during lactate

fermentation is calculated as:

$$Y_{5,3} = \frac{\text{Mass Propionate}}{-\text{Mass Lactate}} = \frac{\text{Mol. Pro} \times \text{MM Pro}}{-\text{Mol. Lac} \times \text{MM Lac}} = \frac{2 \times 74}{-(-10) \times 90} \approx 0.16444$$

where values for stoichiometric coefficients and molar mass are provided in Table 7, and the indices 5 and 3 correspond with the Peterson Matrix shown as Table 10.

Using the described rate equations and derived yield coefficients, the time evolution of material c_i in the resulting *reaction terms* can be written as a set of differential equations in the form:

$$R(c_i) = \dot{c}_i = \sum_{j=1}^{9} Y_{i,j}\phi_j, \tag{14}$$

where variables, processes and indices are as defined in the previous sections and correspond with the Peterson Matrix in Table 10. Analysis of the mass conservation of these reaction terms follows in Section A.4.3.

***e*MT-Model** In [22], the authors extend the ADM1 model to simulate *strains* of biomass within a biomass functional group. These *strains* can be identified within a group based on their specified biochemical reaction parameters. We adapt this idea to extend the MT-model of [19] to consider multiple strains as well, herein referred to as the *e*MT-model of carbohydrate digestion. Biochemical parameters for biomass within a group were generated as follows:

$$P_{i,j} = \mathcal{N}(P_i, \sigma), \tag{15}$$

where $P_{i,j}$ is a biochemical reaction parameters (maximum specific growth rate, half-saturation concentration) for the jth strain of biomass functional group i, chosen randomly from the set of values normally distributed around P_i, the default/set value for the parameter assuming single strain representation, with standard deviation as indicated by σ.

This microbial representation extension can be applied naturally in rate models of fermentation (11) and biomaterial decay (13) as previously defined, as each biomass representative within a functional group has its particular parameter set. However, enzymatic hydrolysis of fiber described by contois kinetics must be modeled as followed:

$$\phi_1 = \frac{I \sum_{j=1}^{n_1} \kappa_{1,j} X_{1,j}}{I + \sum_{j=1}^{n_1} K_{1,j} X_{1,j}}, \tag{16}$$

where indices, variables and parameters are as defined previously.

A.2.2 Component Exchange

The MT-model of [19] also considered separate biochemical environments, the lumen and mucus. Exchange of material **c** occurs between these layers both as active (attachment, absorption, detachment) and passive (diffusion) transport. These exchange terms are all linear and vary based on their directionality.

Attachment (lumen $\rightarrow$ mucus): The active transport of material from the lumen compartment to the mucus compartment. Included materials are lactate, acetate, propionate, butyrate, methane, carbon dioxide, water, and biomass functional groups. This process is modeled as:

$$E_{i,2} = \gamma_{1,i} c_{1,i} \tag{17}$$

Table 6: Derived yield coefficients for components involved in fermentation step 1: Glucose Utilization.

Index *i*	Material	Mol. Count	Mol. Mass [g/mol]	Mass [g]	Yield Coefficient [g/g]
1	**glucose**	-11	180	-1980	-1
	ammonia[a]	-6	17	-102	-0.05152
2	lactate	2	90	180	0.09091
3	hydrogen	6	2	12	0.00606
4	acetate	4	60	240	0.12121
5	propionate	4	74	296	0.14949
6	butyrate	1	88	88	0.04444
7	methane	0	16	0	0
8	carbon dioxide	6	44	264	0.13333
9	water	18	18	324	0.12364
10	Fiber	-	-	-	0
11	SD Biomass	6	113	678	0.3424
12	LD Biomass	0	113	0	0
13	HDA Biomass	0	113	0	0
14	HDM Biomass	0	113	0	0
			Sum:	0	4e-5

a - ammonia sources assumed to be readily available and are not formally tracked in mathematical model.

Table 7: Derived yield coefficients for components involved in fermentation step 2: Lactate Utilization.

Index *i*	Material	Mol. Count	Mol. Mass [g/mol]	Mass [g]	Yield Coefficient [g/g]
1	glucose	0	180	0	0
	ammonia[a]	-3	17	-51	-0.056667
2	**lactate**	-10	90	-900	-1
3	hydrogen	2	2	4	0.00444
4	acetate	1	60	60	0.06667
5	propionate	2	74	148	0.16444
6	butyrate	1	88	88	0.09778
7	methane	0	16	0	0
8	carbon dioxide	3	44	132	0.14667
9	water	10	18	180	0.20000
10	Fiber	-	-	-	0
11	SD Biomass	0	113	0	0
12	LD Biomass	3	113	339	0.37667
13	HDA Biomass	0	113	0	0
14	HDM Biomass	0	113	0	0
			Sum:	0	3e-6

a - ammonia sources assumed to be readily available and are not formally tracked in mathematical model.

Table 8: Derived yield coefficients for components involved in fermentation step 3: Hydrogen Utilizing Acetogenesis.

Index *i*	Material	Mol. Count	Mol. Mass [g/mol]	Mass [g]	Yield Coefficient [g/g]
1	glucose	0	180	0	0
	ammonia[a]	-1	17	-17	-0.60714
2	lactate	0	90	0	0
3	**hydrogen**	-14	2	-28	-1
4	acetate	1	60	60	2.14286
5	propionate	0	74	0	0
6	butyrate	0	88	0	0
7	methane	0	16	0	0
8	carbon dioxide	-7	44	-308	-11.000
9	water	10	18	180	6.42857
10	Fiber	-	-	-	0
11	SD Biomass	0	113	0	0
12	LD Biomass	0	113	0	0
13	HDA Biomass	1	113	113	4.03571
14	HDM Biomass	0	113	0	0
			Sum:	0	0

a - ammonia sources assumed to be readily available and are not formally tracked in mathematical model.

Table 9: Derived yield coefficients for components involved in fermentation step 4: Hydrogen Utilizing Methanogenesis.

Index *i*	Material	Mol. Count	Mol. Mass [g/mol]	Mass [g]	Yield Coefficient [g/g]
1	glucose	0	180	0	0
	ammonia[a]	-1	17	-17	-0.60714
2	lactate	0	90	0	0
3	**hydrogen**	-14	2	-28	-1
4	acetate	0	60	0	0
5	propionate	0	74	0	0
6	butyrate	0	88	0	0
7	methane	1	16	16	0.57143
8	carbon dioxide	-6	44	-264	-9.42857
9	water	10	18	180	6.42857
10	Fiber	-	-	-	0
11	SD Biomass	0	113	0	0
12	LD Biomass	0	113	0	0
13	HDA Biomass	0	113	0	0
14	HDM Biomass	1	113	113	4.035714
			Sum:	0	4e-6

a - ammonia sources assumed to be readily available and are not formally tracked in mathematical model.

Table 10: Peterson Matrix of biochemical/metabolic reaction terms for soluble substrates, polysaccharide carbohydrates and biomass concentrations without biomass strain refinement. Adapted from [19].

For soluble components											
	Component i	1	2	3	4	5	6	7	8	9	**Kinetic Rate**
p_r	**Process**	S_1	S_2	S_3	S_4	S_5	S_6	S_7	S_8	S_9	
1	Hydrolysis	$Y_{1,1}$									$\phi_1(\boldsymbol{c})$
2	Glucose utilization	-1	$Y_{2,2}$	$Y_{3,2}$	$Y_{4,2}$	$Y_{5,2}$	$Y_{6,2}$		$Y_{8,2}$	$Y_{9,2}$	$\phi_2(\boldsymbol{c})$
3	Lactate utilization		-1	$Y_{3,3}$	$Y_{4,3}$	$Y_{5,3}$	$Y_{6,3}$		$Y_{8,3}$	$Y_{9,3}$	$\phi_3(\boldsymbol{c})$
4	Homoacetogenesis			-1	$Y_{4,4}$				$Y_{8,4}$	$Y_{9,4}$	$\phi_4(\boldsymbol{c})$
5	Methanogenesis			-1				$Y_{7,5}$	$Y_{8,5}$	$Y_{9,5}$	$\phi_5(\boldsymbol{c})$

For particulate components							
	Component i	10	11	12	13	14	**Kinetic Rate**
j	**Process**	I_1	X_1	X_2	X_3	X_4	
1	Hydrolysis	-1					$\phi_1(\boldsymbol{c}) = \kappa_1 \frac{I_1 X_1}{K_1 X_1 + I_1}$
2	Glucose utilization		$Y_{11,2}$				$\phi_2(\boldsymbol{c}) = \kappa_2 \frac{S_1 X_1}{K_2 + S_1}$
3	Lactate utilization			$Y_{12,3}$			$\phi_3(\boldsymbol{c}) = \kappa_3 \frac{S_2 X_2}{K_3 + s_2}$
4	Homoacetogenesis				$Y_{13,4}$		$\phi_4(\boldsymbol{c}) = \kappa_4 \frac{S_3 X_3}{K_3 + S_3}$
5	Methanogenesis					$Y_{14,5}$	$\phi_5(\boldsymbol{c}) = \kappa_5 \frac{S_3 X_4}{K_5 + S_3} I_{pH}$ with $I_{pH} = \begin{cases} exp(-3(\frac{pH - pH_U}{pH_U - pH_L})^2) & \text{if } pH < pH_U, \\ 1 & \text{if } pH \geq pH_U \end{cases}$
6	Decay of X_1		-1				$\phi_6(\boldsymbol{c}) = \kappa_{6,1} X_1$
7	Decay of X_2			-1			$\phi_7(\boldsymbol{c}) = \kappa_{7,1} X_2$
8	Decay of X_3				-1		$\phi_8(\boldsymbol{c}) = \kappa_{8,1} X_3$
9	Decay of X_4					-1	$\phi_9(\boldsymbol{c}) = \kappa_{9,1} X_4$

Absorption (mucus → host): The active removal of material from the mucus compartment by the body (lactate, acetate, propionate, butyrate, water) or removal as gas (hydrogen, carbon dioxide). This process is modeled as:

$$E_{i,1} = \gamma_{2,i} c_{2,i} \tag{18}$$

Diffusion (mucus ↔ lumen): The passive transport of material between lumen and mucus compartments. Only sugar undergoes diffusive transport. This process is modeled as:

$$E_{i,3} = \frac{\gamma_{3,i}}{V_l}(c_{1,i} - c_{2,i}) \tag{19}$$

Sloughing/Detachment (mucus → lumen): The active removal f material from the mucus back into the lumen. Materials involved in sloughing include particular fiber and biomass functional groups. This process is modeled as:

$$E_{i,4} = \gamma_{4,i} c_{2,i} \tag{20}$$

The rate of exchange varies from location to location along the length of the colon. Experimental approximations for these exchange rates are taken for the coarsely defined locations of the colon (proximal, transverse, distal). The MT-model applied in [19] considers a 3-stage reactor system physical representation analogous to commonly used *in vitro* systems [14], allowing for easy adaptation of experimentally derived exchange parameter approximations. To model the colon as a continuous system, we interpolate exchange parameters as a function of location x by constructing natural cubic splines approximating parameters as a function of length along the colon, using the algorithm described in [21]. We define transition points and regions, outside of which parameters are treated as they would be discretely. For example, we determine the central transition points to be 14% and 42% along the length of the colon, from proximal to transverse and then transverse to distal, respectively, based on approximate colon dimensions [23], and the region of transition to be 10% (as to prevent overlap of regions). This means that 0-4%, 24-32% and 52-100% inclusive along the length of the colon will take the strict parameters associated with discrete proximal, transverse and distal colons, respectively, while the regions of 4-24%, and 32-52% exclusive will transition between the discrete bounds using the cubic approximation. By constructing these spline functions, we emphasize the lack of obvious representation of physiological colon parameters as a function of space due to unavailability of spatially continuous data.

A.2.3 Transport

As stated previously, we assume that all forces involved in peristaltic movement can be captured in a single *average* flow rate term, which translates to a single convective velocity term

$$F(\mathbf{c}) = \bar{v}\mathbf{c}, \tag{21}$$

where the convective velocity $\bar{v}$ is approximated as:

$$\bar{v} = \begin{cases} 0.001\frac{q}{\pi r^2} & \text{for lumen components} \\ 0 & \text{for mucus components} \end{cases} \tag{22}$$

where q is the average flow rate [L/d] (back-calculated using mean transit times), r is the cross-sectional radius [m], and 0.001 is the metric conversion from litres to cubic meters. As noted in the model assumptions, we treat the colon as a tube with constant cross-sectional radius, meaning the convective velocity is not a

function of location x. And so the full model with convective flux evaluated as a velocity term would take the form:

$$\partial_t \boldsymbol{c} + \bar{v}\partial_x \boldsymbol{c} = R(\boldsymbol{c}) + E(\boldsymbol{c}) \tag{23}$$

We expect that a simple *average flow rate*-type approximation will be suitable when simulating the behaviour of colons exhibiting healthy transit times, implicitly assuming well-mixed material and subsequently equal probability exchange. However, the assumptions of well-mixed material should naturally deteriorate as we move along the colon and the viscosity of digesta increases. Describing the physics of these viscosity changes is a current work in progress.

A.2.4 Endogenous Processes

In our model, we primarily focus on dietary materials and their by-products; effectively disconnecting the colon from other physiological systems. This is seen in the way we account for SCFA absorption as a simple removal term rather than attempting to track its behavior in the body. We do, however, include a description of endogenous mucus production as it is an important stabilizing nutrient source for intestinal microflora. We model the rate of endogenous mucus production Λ as:

$$\Lambda = \Gamma\left(1 - \frac{I_2}{I_M}\right), \tag{24}$$

where I_2 is the fiber of polysaccharides in the mucus environment, Γ is the maximum endogenous mucus production rate [g/Ld], and I_M is the maximum/critical density of fiber in the mucus environment. Including further endogenous processes, namely transport of material from the blood stream into the colon, is a potential model extension.

A.3 Complete Model

The complete model can be formulated by combining the previously described reaction, exchange and flow processes. To avoid any ambiguity, we write out all partial differential equations that compose the model.

Lumen Components:

Sugar ($S_{1,1}$):

$$\begin{aligned}
\partial_t S_{1,1} + \bar{v}_l \partial_x S_{1,1} = \quad & Y_{1,1}\frac{I_{1,1}\sum_j^{n_1}\kappa_{1,j}X_{1,1,j}}{\left(\sum_j^{n_1} K_{1,j}X_{1,1,j}\right) + I_{1,1}} && \text{hydrolysis}\\
& - \sum_j^{n_1}\frac{\kappa_{2,j}S_{1,1}X_{1,1,j}}{K_{2,j}+S_{1,1}} && \text{sugar utilization}\\
& - \frac{\gamma_{3,1}}{V_l}(S_{1,1} - S_{2,1}) && \text{diffusion}
\end{aligned}$$

Lactate ($S_{1,2}$):

$$\begin{aligned}
\partial_t S_{1,2} + \bar{v}_l \partial_x S_{1,2} = \quad & Y_{2,2}\sum_j^{n_1}\frac{\kappa_{2,j}S_{1,1}X_{1,1,j}}{K_{2,n_1}+S_{1,1}} && \text{sugar utilization}\\
& - \sum_j^{n_2}\frac{\kappa_{3,j}S_{1,2}X_{1,2,j}}{K_{3,j}+S_{1,2}} && \text{lactate utilization}\\
& - \gamma_{1,2}S_{1,2} && \text{attachment}
\end{aligned}$$

Hydrogen ($S_{1,3}$):

$$\begin{aligned}
\partial_t S_{1,3} + \bar{v}_l \partial_x S_{1,3} = \quad & Y_{3,2} \sum_{n_1}^{N_1} \frac{\kappa_{2,n_1} S_{1,1} X_{1,1_{n_1}}}{K_{2,n_1} + S_{1,1}} && \text{sugar utilization} \\
& + Y_{3,3} \sum_{n_2}^{N_2} \frac{\kappa_{3,n_2} S_{1,2} X_{1,2_{n_2}}}{K_{3,n_2} + S_{1,2}} && \text{lactate utilization} \\
& - \sum_{n_3}^{N_3} \frac{\kappa_{4,n_3} S_{1,3} X_{1,3_{n_3}}}{K_{4,n_3} + S_{1,3}} && \text{acetogenesis} \\
& - \sum_{n_3}^{N_3} \frac{\kappa_{5,n_3} S_{1,3} X_{1,4_{n_4}}}{K_{5,n_4} + S_{1,3}} I_{pH}(x) && \text{methanogenesis}
\end{aligned}$$

Acetate ($S_{1,4}$):

$$\begin{aligned}
\partial_t S_{1,4} + \bar{v}_l \partial_x S_{1,4} = \quad & Y_{4,2} \sum_{n_1}^{N_1} \frac{\kappa_{2,n_1} S_{1,1} X_{1,1_{n_1}}}{K_{2,n_1} + S_{1,1}} && \text{sugar utilization} \\
& + Y_{4,3} \sum_{n_2}^{N_2} \frac{\kappa_{3,n_2} S_{1,2} X_{1,2_{n_2}}}{K_{3,n_2} + S_{1,2}} && \text{lactate utilization} \\
& + Y_{4,4} \sum_{n_3}^{N_3} \frac{\kappa_{4,n_3} S_{1,3} X_{1,3_{n_3}}}{K_{4,n_3} + S_{1,3}} && \text{acetogenesis} \\
& - \gamma_{1,4} S_{1,4} && \text{attachment}
\end{aligned}$$

Propionate ($S_{1,5}$):

$$\begin{aligned}
\partial_t S_{1,5} + \bar{v}_l \partial_x S_{1,5} = \quad & Y_{5,2} \sum_{n_1}^{N_1} \frac{\kappa_{2,n_1} S_{1,1} X_{1,1_{n_1}}}{K_{2,n_1} + S_{1,1}} && \text{sugar utilization} \\
& + Y_{5,3} \sum_{n_2}^{N_2} \frac{\kappa_{3,n_2} S_{1,2} X_{1,2_{n_2}}}{K_{3,n_l} + S_{1,2}} && \text{lactate utilization} \\
& - \gamma_{1,5} S_{1,5} && \text{attachment}
\end{aligned}$$

Butyrate ($S_{1,6}$):

$$\begin{aligned}
\partial_t S_{1,6} + \bar{v}_l \partial_x S_{1,6} = \quad & Y_{6,2} \sum_{n_1}^{N_1} \frac{\kappa_{2,n_1} S_{1,1} X_{1,1_{n_1}}}{K_{2,n_1} + S_{1,1}} && \text{sugar utilization} \\
& + Y_{6,3} \sum_{n_2}^{N_2} \frac{\kappa_{3,n_2} S_{1,2} X_{1,2_{n_2}}}{K_{3,n_2} + S_{1,2}} && \text{lactate utilization} \\
& - \gamma_{1,6} S_{1,6} && \text{attachment}
\end{aligned}$$

Methane ($S_{1,7}$):

$$\begin{aligned}
\partial_t S_{1,7} + \bar{v}_l \partial_x S_{1,7} = \quad & Y_{7,5} \sum_{n_4}^{N_4} \frac{\kappa_{5,n_2} S_{1,3} X_{1,4_{n_4}}}{K_{5,n_4} + S_{1,3}} I_{pH}(x) && \text{methanogenesis} \\
& - \gamma_{1,7} S_{1,7} && \text{attachment}
\end{aligned}$$

Carbon dioxide ($S_{1,8}$):

$$\begin{aligned}
\partial_t S_{1,8} + \bar{v}_l \partial_x S_{1,8} = \quad & Y_{8,2} \sum_{n_1}^{N_1} \frac{\kappa_{2,n_1} S_{1,1} X_{1,1_{n_1}}}{K_{2,n_1} + S_{1,1}} && \text{sugar utilization} \\
& + Y_{8,3} \sum_{n_2}^{N_2} \frac{\kappa_{3,n_2} S_{1,2} X_{1,2_{n_2}}}{K_{3,n_2} + S_{1,2}} && \text{lactate utilization} \\
& + Y_{8,4} \sum_{n_3}^{N_3} \frac{\kappa_{4,n_3} S_{1,3} X_{1,3_{n_3}}}{K_{4,n_3} + S_{1,3}} && \text{acetogenesis} \\
& + Y_{8,5} \sum_{n_4}^{N_4} \frac{\kappa_{5,n_4} S_{1,3} X_{1,4_{n_4}}}{K_{5,n_4} + S_{1,3}} I_{pH}(x) && \text{methanogenesis} \\
& - \gamma_{1,8} S_{1,8} && \text{attachment}
\end{aligned}$$

Water ($S_{1,9}$):

$$\begin{aligned}
\partial_t S_{1,9} + \bar{v}_l \partial_x S_{1,9} = \quad & Y_{9,2} \sum_{n_1}^{N_1} \frac{\kappa_{2,n_1} S_{1,1} X_{1,1_{n_1}}}{K_{2,n_1} + S_{1,1}} && \text{sugar utilization} \\
& + Y_{9,3} \sum_{n_2}^{N_2} \frac{\kappa_{3,n_2} S_{1,2} X_{1,2_{n_2}}}{K_{3,n_2} + S_{1,2}} && \text{lactate utilization} \\
& + Y_{9,4} \sum_{n_3}^{N_3} \frac{\kappa_{4,n_3} S_{1,3} X_{1,3_{n_3}}}{K_{4,n_3} + S_{1,3}} && \text{acetogenesis} \\
& + Y_{9,5} \sum_{n_4}^{N_4} \frac{\kappa_{5,n_4} S_{1,3} X_{1,4_{n_4}}}{K_{5,n_4} + S_{1,3}} I_{pH}(x) && \text{methanogenesis} \\
& - \gamma_{1,9} S_{1,9} && \text{attachment}
\end{aligned}$$

Fiber ($I_{1,1}$):

$$\begin{aligned}
\partial_t I_{1,1} + \bar{v}_l \partial_x I_{1,1} = & - \frac{I_{1,1} \sum_{n_1}^{N_1} \kappa_{1,n_1} Y_{1,1,n_1} X_{1,n_1}}{\left(\sum_{n_1}^{N_1} K_{1,n_1} X_{1,1_{n_1}} \right) + I_{1,1}} && \text{hydrolysis} \\
& + \left(\frac{V_m}{V_l} \right) \gamma_{4,10} I_{2,1} && \text{sloughing}
\end{aligned}$$

Sugar Degraders ($X_{1,1,n_1}$):

$$\begin{aligned}
\forall n_1 \leq N_1 : \partial_t X_{1,1_{n_1}} + \bar{v}_l \partial_x X_{1,1_{n_1}} = \quad & Y_{11,2} \frac{\kappa_{2,n_1} S_{1,1} X_{1,1_{n_1}}}{K_{2,n_1} + S_{1,1}} && \text{sugar utilization} \\
& - \gamma_{1,11_{n_1}} X_{1,1_{n_s}} && \text{attachment} \\
& + \left(\frac{V_m}{V_l} \right) \gamma_{4,11_{n_1}} X_{2,11_{n_1}} && \text{sloughing} \\
& - \kappa_{6,n_1} X_{1,1_{n_s}} && \text{decay}
\end{aligned}$$

Lactate Degraders ($X_{1,2,n_2}$):

$$\begin{aligned}
\forall n_2 \leq N_2 : \partial_t X_{1,2_{n_2}} + \bar{v}_l \partial_x X_{1,2_{n_2}} = \quad & Y_{12,3} \frac{\kappa_{3,n_2} S_{1,2} X_{1,2_{n_2}}}{K_{3,n_2} + S_{1,2}} && \text{lactate utilization} \\
& - \gamma_{1,12_{n_2}} X_{1,2_{n_l}} && \text{attachment} \\
& + \left(\frac{V_m}{V_l}\right) \gamma_{4,12_{n_2}} X_{2,2_{n_2}} && \text{sloughing} \\
& - \kappa_{7,n_2} X_{1,2_{n_2}} && \text{decay}
\end{aligned}$$

Hydrogen Degrading Acetogens ($X_{1,3,n_3}$):

$$\begin{aligned}
\forall n_3 \leq N_3 : \partial_t X_{1,3_{n_3}} + \bar{v}_l \partial_x X_{1,3_{n_3}} = \quad & Y_{13,4} \frac{\kappa_{4,n_3} S_{1,3} X_{1,3_{n_3}}}{K_{4,n_4} + S_{1,3}} && \text{acetogenesis} \\
& - \gamma_{1,13_{n_3}} X_{1,3_{n_3}} && \text{attachment} \\
& + \left(\frac{V_m}{V_l}\right) \gamma_{4,13_{n_3}} X_{2,3_{n_3}} && \text{sloughing} \\
& - \kappa_{8,n_3} X_{1,3_{n_3}} && \text{decay}
\end{aligned}$$

Hydrogen Degrading Methanogens ($X_{1,4,n_4}$):

$$\begin{aligned}
\forall n_4 \leq N_4 : \partial_t X_{1,4_{n_4}} + \bar{v}_l \partial_x X_{1,4_{n_4}} = \quad & Y_{14,5} \frac{\kappa_{5,n_4} S_{1,3} X_{1,4_{n_4}}}{K_{5,n_4} + S_{1,3}} && \text{methanogenesis} \\
& - \gamma_{1,14_{n_4}} X_{1,4_{n_4}} && \text{attachment} \\
& + \left(\frac{V_m}{V_l}\right) \gamma_{4,14_{n_4}} X_{2,4_{n_4}} && \text{sloughing} \\
& - \kappa_{9,n_4} X_{1,4_{n_4}} && \text{decay}
\end{aligned}$$

Mucus Components:

Sugar ($S_{2,1}$):

$$\begin{aligned}
\partial_t S_{2,1} = \quad & Y_{1,1} \frac{I_{2,1} \sum_{n_1}^{N_1} \kappa_{1,n_1} X_{2,n_1}}{\left(\sum_{n_1}^{N_1} K_{1,n_1} X_{2,1_{n_1}}\right) + I_{2,1}} && \text{hydrolysis} \\
& - \sum_{n_1}^{N_1} \frac{\kappa_{2,n_1} S_{2,1} X_{2,1_{n_1}}}{K_{2,n_1} + S_{2,1}} && \text{sugar utilization} \\
& + \frac{\gamma_{3,1}}{V_m} (S_{1,1} - S_{2,1}) && \text{diffusion}
\end{aligned}$$

Lactate ($S_{2,2}$):

$$\begin{aligned}
\partial_t S_{2,2} = \quad & Y_{2,2} \sum_{n_1}^{N_1} \frac{\kappa_{2,n_1} S_{2,1} X_{2,1_{n_1}}}{K_{2,n_1} + S_{2,1}} && \text{sugar utilization} \\
& - \sum_{n_2}^{N_2} \frac{\kappa_{3,n_2} S_{2,2} X_{2,2_{n_2}}}{K_{3,n_2} + S_{2,2}} && \text{lactate utilization} \\
& + \left(\frac{V_l}{V_m}\right) \gamma_{1,2} S_{1,2} && \text{attachment} \\
& - \gamma_{2,2} S_{2,2} && \text{absorption}
\end{aligned}$$

Hydrogen ($S_{2,3}$):

$$\begin{aligned}
\partial_t S_{2,3} = \quad & Y_{3,2} \sum_{n_1}^{N_1} \frac{\kappa_{2,n_1} S_{2,1} X_{2,1_{n_1}}}{K_{2,n_1} + S_{2,1}} && \text{sugar utilization} \\
& + Y_{3,3} \sum_{n_2}^{N_2} \frac{\kappa_{3,n_2} S_{2,2} X_{2,2_{n_2}}}{K_{3,n_2} + S_{2,2}} && \text{lactate utilization} \\
& - \sum_{n_3}^{N_3} \frac{\kappa_{4,n_3} S_{2,3} X_{2,3_{n_3}}}{K_{4,n_3} + S_{2,3}} && \text{acetogenesis} \\
& - \sum_{n_3}^{N_3} \frac{\kappa_{5,n_3} S_{2,3} X_{2,4_{n_4}}}{K_{5,n_4} + S_{2,3}} I_{pH}(x) && \text{methanogenesis}
\end{aligned}$$

Acetate ($S_{2,4}$):

$$\begin{aligned}
\partial_t S_{2,4} = \quad & Y_{4,2} \sum_{n_1}^{N_1} \frac{\kappa_{2,n_1} S_{2,1} X_{2,1_{n_1}}}{K_{2,n_1} + S_{2,1}} && \text{sugar utilization} \\
& + Y_{4,3} \sum_{n_2}^{N_2} \frac{\kappa_{3,n_2} S_{2,2} X_{2,2_{n_2}}}{K_{3,n_2} + S_{2,2}} && \text{lactate utilization} \\
& + Y_{4,4} \sum_{n_3}^{N_3} \frac{\kappa_{4,n_3} S_{2,3} X_{2,3_{n_3}}}{K_{4,n_3} + S_{2,3}} && \text{acetogenesis} \\
& + \left(\frac{V_l}{V_m} \right) \gamma_{1,4} S_{1,4} && \text{attachment} \\
& - \gamma_{2,4} S_{2,4} && \text{absorption}
\end{aligned}$$

Propionate ($S_{2,5}$):

$$\begin{aligned}
\partial_t S_{2,5} = \quad & Y_{5,2} \sum_{n_1}^{N_1} \frac{\kappa_{2,n_1} S_{2,1} X_{1,1_{n_1}}}{K_{2,n_1} + S_{2,1}} && \text{sugar utilization} \\
& + Y_{5,3} \sum_{n_2}^{N_2} \frac{\kappa_{3,n_2} S_{2,2} X_{2,2_{n_2}}}{K_{3,n_l} + S_{2,2}} && \text{lactate utilization} \\
& + \left(\frac{V_l}{V_m} \right) \gamma_{1,5} S_{1,5} && \text{attachment} \\
& - \gamma_{2,5} S_{2,5} && \text{absorption}
\end{aligned}$$

Butyrate ($S_{2,6}$):

$$\begin{aligned}
\partial_t S_{2,6} = \quad & Y_{6,2} \sum_{n_1}^{N_1} \frac{\kappa_{2,n_1} S_{2,1} X_{2,1_{n_1}}}{K_{2,n_1} + S_{2,1}} && \text{sugar utilization} \\
& + Y_{6,3} \sum_{n_2}^{N_2} \frac{\kappa_{3,n_2} S_{2,2} X_{2,2_{n_2}}}{K_{3,n_2} + S_{2,2}} && \text{lactate utilization} \\
& + \left(\frac{V_l}{V_m} \right) \gamma_{1,6} S_{1,6} && \text{attachment} \\
& - \gamma_{2,6} S_{2,6} && \text{absorption}
\end{aligned}$$

Methane ($S_{2,7}$):

$$\begin{aligned}
\partial_t S_{2,7} = \quad & Y_{7,5} \sum_{n_4}^{N_4} \frac{\kappa_{5,n_2} S_{2,3} X_{2,4_{n_4}}}{K_{5,n_4} + S_{2,3}} I_{pH}(x) && \text{methanogenesis} \\
& + \left(\frac{V_l}{V_m} \right) \gamma_{1,7} S_{1,7} && \text{attachment} \\
& - \gamma_{2,7} S_{2,7} && \text{absorption}
\end{aligned}$$

Carbon dioxide ($S_{2,8}$):

$$\begin{aligned}
\partial_t S_{2,8} = & Y_{8,2} \sum_{n_1}^{N_1} \frac{\kappa_{2,n_1} S_{2,1} X_{2,1_{n_1}}}{K_{2,n_1} + S_{2,1}} && \text{sugar utilization} \\
& + Y_{8,3} \sum_{n_2}^{N_2} \frac{\kappa_{3,n_2} S_{2,2} X_{2,2_{n_2}}}{K_{3,n_2} + S_{2,2}} && \text{lactate utilization} \\
& + Y_{8,4} \sum_{n_3}^{N_3} \frac{\kappa_{4,n_3} S_{2,3} X_{2,3_{n_3}}}{K_{4,n_3} + S_{2,3}} && \text{acetogenesis} \\
& + Y_{8,5} \sum_{n_4}^{N_4} \frac{\kappa_{5,n_4} S_{2,3} X_{2,4_{n_4}}}{K_{5,n_4} + S_{2,3}} I_{pH}(x) && \text{methanogenesis} \\
& + \left(\frac{V_l}{V_m} \right) \gamma_{1,8} S_{1,8} && \text{attachment} \\
& - \gamma_{2,8} S_{2,8} && \text{absorption}
\end{aligned}$$

Water ($S_{2,9}$):

$$\begin{aligned}
\partial_t S_{2,9} = \quad & Y_{9,2} \sum_{n_1}^{N_1} \frac{\kappa_{2,n_1} S_{2,1} X_{2,1_{n_1}}}{K_{2,n_1} + S_{2,1}} && \text{sugar utilization} \\
& + Y_{9,3} \sum_{n_2}^{N_2} \frac{\kappa_{3,n_2} S_{2,2} X_{2,2_{n_2}}}{K_{3,n_2} + S_{2,2}} && \text{lactate utilization} \\
& + Y_{9,4} \sum_{n_3}^{N_3} \frac{\kappa_{4,n_3} S_{2,3} X_{2,3_{n_3}}}{K_{4,n_3} + S_{2,3}} && \text{acetogenesis} \\
& + Y_{9,5} \sum_{n_4}^{N_4} \frac{\kappa_{5,n_4} S_{2,3} X_{2,4_{n_4}}}{K_{5,n_4} + S_{2,3}} I_{pH}(x) && \text{methanogenesis} \\
& + \left(\frac{V_l}{V_m} \right) \gamma_{1,9} S_{1,9} && \text{attachment} \\
& - \gamma_{2,9} S_{2,9} && \text{absorption}
\end{aligned}$$

Mucins ($I_{2,1}$):

$$\begin{aligned}
\partial_t I_{2,1} = \quad & \Lambda && \text{endogenous production} \\
& - \frac{I_{2,1} \sum_{n_1}^{N_1} \kappa_{1,n_1} Y_{1,1} X_{2,n_1}}{\left(\sum_{n_1}^{N_1} K_{1,n_1} X_{2,1_{n_1}} \right) + I_{2,1}} && \text{hydrolysis} \\
& - \gamma_{4,10} I_{2,1} && \text{sloughing}
\end{aligned}$$

Sugar Degraders ($X_{2,1,n_1}$):

$$\begin{aligned}\forall n_1 \leq N_1 : \partial_t X_{2,1_{n_1}} = \quad & Y_{11,2}\frac{\kappa_{2,n_1} S_{2,1} X_{2,1_{n_1}}}{K_{2,n_1} + S_{2,1}} && \text{sugar utilization} \\ & + \left(\frac{V_l}{V_m}\right)\gamma_{1,11_{n_1}} X_{1,1_{n_s}} && \text{attachment} \\ & - \gamma_{4,11_{n_1}} X_{2,11_{n_1}} && \text{sloughing} \\ & - \kappa_{6,n_1} X_{2,1_{n_s}} && \text{decay}\end{aligned}$$

Lactate Degraders ($X_{2,2,n_2}$):

$$\begin{aligned}\forall n_2 \leq N_2 : \partial_t X_{2,2_{n_2}} + \bar{v}_l \partial_x X_{2,2_{n_2}} = \quad & Y_{12,3}\frac{\kappa_{3,n_2} S_{2,2} X_{2,2_{n_2}}}{K_{3,n_2} + S_{2,2}} && \text{lactate utilization} \\ & + \left(\frac{V_l}{V_m}\right)\gamma_{1,12_{n_2}} X_{1,2_{n_l}} && \text{attachment} \\ & - \gamma_{4,12_{n_2}} X_{2,2_{n_2}} && \text{sloughing} \\ & - \kappa_{7,n_2} X_{2,2_{n_2}} && \text{decay}\end{aligned}$$

Hydrogen Degrading Acetogens ($X_{2,3,n_3}$):

$$\begin{aligned}\forall n_3 \leq N_3 : \partial_t X_{2,3_{n_3}} + \bar{v}_l \partial_x X_{2,3_{n_3}} = \quad & Y_{13,4}\frac{\kappa_{4,n_3} S_{2,3} X_{2,3_{n_3}}}{K_{4,n_4} + S_{2,3}} && \text{acetogenesis} \\ & + \left(\frac{V_l}{V_m}\right)\gamma_{1,13_{n_3}} X_{1,3_{n_3}} && \text{attachment} \\ & + \gamma_{4,13_{n_3}} X_{2,3_{n_3}} && \text{sloughing} \\ & - \kappa_{8,n_3} X_{2,3_{n_3}} && \text{decay}\end{aligned}$$

Hydrogen Degrading Methanogens ($X_{2,4,n_4}$):

$$\begin{aligned}\forall n_4 \leq N_4 : \partial_t X_{2,4_{n_4}} + \bar{v}_l \partial_x X_{2,4_{n_4}} = \quad & Y_{14,5}\frac{\kappa_{5,n_4} S_{2,3} X_{2,4_{n_4}}}{K_{5,n_4} + S_{2,3}} && \text{methanogenesis} \\ & + \left(\frac{V_l}{V_m}\right)\gamma_{1,14_{n_4}} X_{1,4_{n_4}} && \text{attachment} \\ & - \gamma_{4,14_{n_4}} X_{2,4_{n_4}} && \text{sloughing} \\ & - \kappa_{9,n_4} X_{2,4_{n_4}} && \text{decay}\end{aligned}$$

A.4 Numerical Treatment and Considerations

The described continuous model takes a structure similar to many transport models with reactions seen in Chemical Engineering problems. The combination of both non-linear reaction terms and linear exchange terms between a fluid and stationary medium creates individual processes proceeding at different time scales, creating significant stiffness in the source terms. To integrate our stiff model, we apply a central scheme for balance laws as described in [12]. To begin, we re-write model (1) by:

$$c_t + f(c)_x = g(c) \tag{25}$$

where $f(c)$ is the flux of material (simply first-order convection in our model), and $g(c)$ is representative of stiff source terms, as to follow the standards presented in [12].

To solve numerically, we discretize Equation (25) in both space and time:

$$\Delta x = \frac{L}{N+1}, \qquad \Delta t <= \frac{\Delta x}{2\bar{v}},$$

where L is the length of the colon, and N is the number of grid points used to discretize the continuous length. The resulting discrete representation of the model (25) is presented as:

$$\begin{aligned} u_{\chi+1/2}^{\tau+1} &= \tfrac{1}{2}\left(u_{\chi}^{\tau} + u_{\chi+1}^{\tau}\right) + \tfrac{1}{8}\left(u'_{\chi} - u'_{\chi+1}\right) - \tfrac{\Delta t}{\Delta x}\left(f(u_{\chi+1}^{\tau+1/2}) - f(u_{\chi}^{\tau+1/2})\right) \\ &+ \Delta t\left(\tfrac{3}{8}g(u_{\chi}^{\tau+1/3}) + \tfrac{3}{8}g(u_{\chi+1}^{\tau+1/3}) + \tfrac{1}{4}g(u_{\chi+1/2}^{\tau+1})\right), \end{aligned} \tag{26}$$

where u_{χ}^{τ} is the approximate concentration of measured quantity [g/L] at the index τ time step and index χth location. Equation (26) solves for concentration $u_{\chi+1/2}^{\tau+1}$ at the current time index $(\tau+1)$ on a staggered grid (center of grid nodes), requiring previous (time level τ) and intermediate (time level $\tau+1/3$, $\tau+1/2$) solutions at the edge of grid nodes. Model (26) is then a system of nonlinear equations that requires iterative solving.

Values at intermediate time levels, $u_{\chi}^{\tau+1/2}$ and $u_{\chi}^{\tau+1/3}$, are solved using an implicit fractional step:

$$\begin{aligned} u_{\chi}^{\tau+1/2} &= u_{\chi}^{\tau} + \tfrac{\Delta t}{2}\left(g(u_{\chi}^{\tau+1/2}) - \tfrac{f'_j}{\Delta x}\right), \\ u_{\chi}^{\tau+1/3} &= u_{\chi}^{\tau} + \tfrac{\Delta t}{3}\left(g(u_{\chi}^{\tau+1/3}) - \tfrac{f'_{\chi}}{\Delta x}\right), \end{aligned}$$

and the values of u'_{χ} and f'_{χ} are first order approximation of the spatial derivatives of the field and the flux, respectively. As in [12], we employ the following flux-limiter treatment:

$$\begin{aligned} u'_{\chi} &= \text{MM}(u_{\chi+1} - u_{\chi} - \tfrac{1}{2}D_{\chi+\frac{1}{2}}u, u_{\chi} - u_{\chi-1} + \tfrac{1}{2}D_{\chi-\frac{1}{2}}u), \quad \text{where} \\ D_{\chi+\frac{1}{2}}u &= \text{MM}(u_{\chi+2} - 2u_{\chi+1} + u_{\chi}, u_{\chi+1} - 2u_{\chi} + u_{\chi-1}), \quad \text{and} \\ \text{MM}(x,y) &= \begin{cases} \text{sgn}(x)\cdot\min(|x|,|y|) & \text{if sgn}(x) = \text{sgn}(y), \\ 0 & \text{otherwise.} \end{cases} \end{aligned}$$

to approximate spatial derivatives. In summary, the approximate solution at the current time step requires the evaluations of 5 non-linear problems using the previous solution at 6 discrete edges (3 on either side).

A.4.1 Boundary Conditions

To complete the model, boundary conditions must be specified at the upstream end of the lumen for all dependent variables. These boundary values are analogous to the bolus composition and frequency entering the large intestine.

Because we do not explicitly model the pre-colon processes, we make use of a *black-box* representation of the upper-GI tract, modeling the transport of dietary input from mouth to colon as a sequence of dilution units. This process effectively buffers sharp input conditions, which is appropriate when considering the pathway of dietary inputs traveling through the GI-tract to the colon. A sequence of dilution units is modeled as:

$$\dot{u_1} = D(u_o - u_1) \quad \text{for first unit} \tag{27}$$

$$\dot{u_k} = D(u_{k-1} - u_i) \quad \text{for sequential units} \tag{28}$$

where D is the dilution rate found using the system flow rate and an approximate volume of pre-colon organs, and u_i is the density of material [g/L] in vessel k, with the density from the final dilution reservoir being the input to the colon model. We define the initial density into the first dilution unit u_o as a periodic piece-wise impulse function, representative of a feeding pattern. Figure 9 demonstrates the effect of dilution treatment on an impulsive diet regiment.

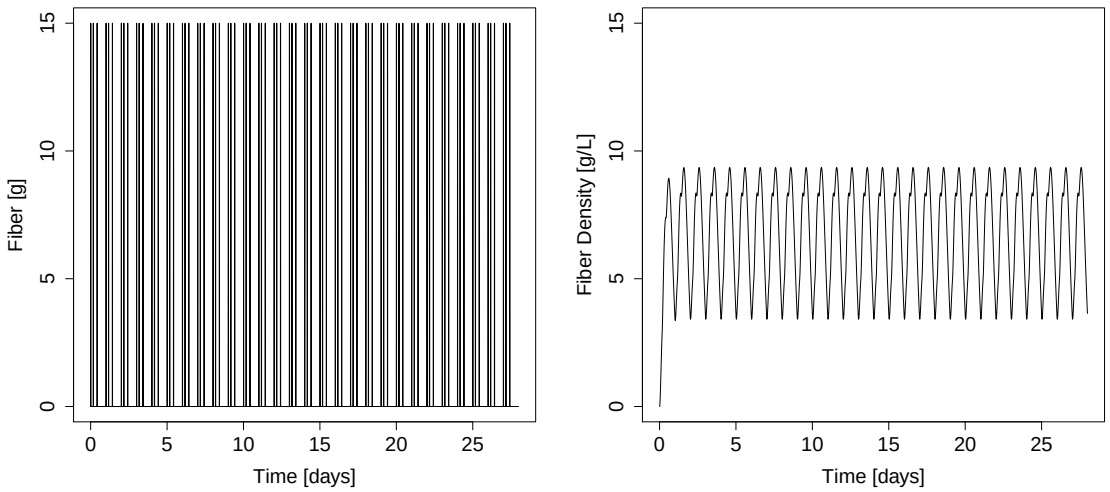

(a) Dietary Input

(b) Colon Boundary Condition

Figure 9: Effect of black-box treatment on periodic impulsed diet (3 x 15g per day, at hour 0, 4, 10 every 24 hours).

A.4.2 Numerical Implementation

The developed mathematical model of variable problem-size and functionally defined sub-processes presents significant organizational challenges during numerical simulation. Additionally, simulation of large models will invariably create large data-sets, both with analytical and visualization challenges. The compuGUT software project stems from these design challenges, providing interested users a preliminary model implementation for review and experimentation [17](Chapter 4). Source codes, user-friendly operation and visualization scripts, additional files and resources, as well as pre-compiled 32 and 64bit Linux binaries are available under GNUv3 licensing at compugut.sourceforge.net.

A.4.3 Numerical Verification

Mass Conservation: The employed numerical scheme [12] is designed to conserve mass. However, the scheme may be unreliable if the digestion sub-model included in the compuGUT is itself not mass conservative. To confirm mass conservation of the digestion sub-model, numerical simulations of the model were executed. These simulations were conducted under *batch* operation assumptions (no input or output of mass), and natural decay/death of biomass is not considered. As such, the total mass of material initializing the system must equal the total mass of material at steady state. The results of this simulation scenario are presented in Table 11.

The difference between final and initial mass is 3.03 grams. The ammonia necessary for this set of reactions to proceed given the initial fiber mass is 3.201 grams of ammonia. Therefore, 0.171 grams, or 0.2%, of unidentified material is lost during calculations. This mass lost in the system can be attributed to computational precision (rounding and truncation errors).

Table 11: Verification of mass conservation

Material	Initial Mass [g]	Final Mass [g]	Difference [g]
glucose	0	0	0
lactate	0	0	0
hydrogen	0	0	0
acetate	0	6.826067	6.826067
propionate	0	8.221962	8.221962
butyrate	0	2.666459	2.666459
methane	0	0.061338	0.061338
carbon dioxide	0	3.946864	3.946864
water	0	11.168698	11.168698
fiber	50	0	-50
SD Biomass	10	27.120000	17.120000
LD Biomass	8	9.712153	1.712153
HDA Biomass	2	2.871074	0.871074
HDM Biomass	0.5	0.935495	0.435495
Total	70.5	73.53011	**3.03011**

Spatial Discretization Errors: To verify the convergence and efficiency of the numerical implementation describing the complete spatially extended model, we perform a grid refinement study. The grid level, or number of discrete representations of the colon length, is given by:

$$N = 50 \times 2^g + 1, \qquad g \in [0, 1, ...5], \tag{29}$$

where g is the grid index, used to systematically generate comparable grids. Simulations were undertaken at every grid level, with continuous input conditions (versus impulsive diets discussed previously) for convenience. Additionally, simulations were run with single-species representations of each biomass group (MT-model of carbohydrate digestion) with default parameters.

Convergence is assessed by comparing the output of all dependent variables at the colon output at a specific time in the simulation (≈ 6.35 days). For ease-of-presentation, we include only the concentration of sugar utilizing biomass in Table 12. Additionally, convergence order is assessed by calculating the rate of error reduction, θ, between solutions of sequential grid resolutions as follows:

$$\theta = \frac{\left|\left|1 - \frac{f_e(X_{g+1})}{f_e(X_\infty)}\right|\right|_2}{\left|\left|1 - \frac{f_e(X_g)}{f_e(X_\infty)}\right|\right|_2}, \qquad g \in [0, 1, .., 4], \tag{30}$$

where X_g is an array of concentrations of all dependent variables at all locations for the specified grid index (g) and at the specified time (≈ 6.35 days), X_∞ is an array of concentrations of all dependent variables at the highest grid level (6), and $f_e(X)$ is an extrapolation function, taking the solutions of X at the 51 locations of the coarse most discretization scheme. The result of this convergence-order assessment is highlighted in Table 12.

In addition to the refinement study, evaluation of the implementation with test scenarios were assessed for accuracy and consistency through repeated simulations.

Table 12: Summary of simulation results for changing grid index, g, giving total number of grid points, N. Sugar Degrading Biomass Density (SDBD) converges towards approximately 27.75 g/L at colon output, with first-order convergence (using rate of error reduction).

g	N	SDBD [g/L]	Relative Error
0	51	13.65207	0.005
1	101	13.61938	0.002
2	201	13.60245	0.001
3	401	13.59373	6e(-4)
4	801	13.58926	3e(-4)
5	1601	13.58696	9e(-5)
6	3201	13.58579	

A.5 Concluding Remarks

The mathematical model as constructed is a highly simplified representation of physiological mechanisms and system interplay in the colon, but uses assumptions regarding continuous flow, component exchange, and mucus representation that are comparable to *in vitro* systems currently employed in gut microflora experimentation [13, 20].

Additionally, the modeling framework is flexible and extensible, thus can be adapted to model a variety of input and initial conditions, and further refined as more complete knowledge about physiological sub-processes is acquired.

References

[1] BATSTONE, D. Mathematical modelling of anaerobic reactors treating domestic wastewater: Rational criteria for model use. *Reviews in Environmental Science and Biotechnology 5*, 1 (2006), 57–71.

[2] BATSTONE, D., KELLER, J., ANGELIDAKI, I., KALYUZHNYI, S., PAVLOSTATHIS, S., ROZZI, A., SANDERS, W., SIEGRIST, H., AND VAVILIN, V. The iwa anaerobic digestion model no 1(adm 1). *Water Science & Technology 45*, 10 (2002), 65–73.

[3] CLEMENTE, J. C., URSELL, L. K., PARFREY, L. W., AND KNIGHT, R. The impact of the gut microbiota on human health: an integrative view. *Cell 148*, 6 (2012), 1258–1270.

[4] CUMMINGS, J., AND MACFARLANE, G. The control and consequences of bacterial fermentation in the human colon. *Journal of Applied Bacteriology 70*, 6 (1991), 443–459.

[5] EASTMAN, J. A., AND FERGUSON, J. F. Solubilization of particulate organic carbon during the acid phase of anaerobic digestion. *Journal (Water Pollution Control Federation)* (1981), 352–366.

[6] GESMANN, M., AND DE CASTILLO, D. Using the google visualisation api with r. *The R Journal 3*, 2 (2011), 40–44.

[7] GUSAKOV, A., SINITSYN, A., AND KLYOSOV, A. Kinetics of the enzymatic hydrolysis of cellulose: 1. a mathematical model for a batch reactor process. *Enzyme and microbial technology 7*, 7 (1985), 346–352.

[8] HELANDER, H. F., AND FÄNDRIKS, L. Surface area of the digestive tract-revisited. *Scandinavian journal of gastroenterology 49*, 6 (2014), 681–689.

[9] HESTER, R. L., ILIESCU, R., SUMMERS, R., AND COLEMAN, T. G. Systems biology and integrative physiological modelling. *The Journal of physiology 589*, 5 (2011), 1053–1060.

[10] HINDMARSH, A. C., BROWN, P. N., GRANT, K. E., LEE, S. L., SERBAN, R., SHUMAKER, D. E., AND WOODWARD, C. S. Sundials: Suite of nonlinear and differential/algebraic equation solvers. *ACM Transactions on Mathematical Software (TOMS) 31*, 3 (2005), 363–396.

[11] KALMOKOFF, M., ZWICKER, B., O'HARA, M., MATIAS, F., GREEN, J., SHASTRI, P., GREEN-JOHNSON, J., AND BROOKS, S. P. Temporal change in the gut community of rats fed high amylose cornstarch is driven by endogenous urea rather than strictly on carbohydrate availability. *Journal of applied microbiology* (2013).

[12] LIOTTA, S. F., ROMANO, V., AND RUSSO, G. Central schemes for balance laws of relaxation type. *SIAM Journal on Numerical Analysis 38*, 4 (2000), 1337–1356.

[13] MACFARLANE, G. T., AND MACFARLANE, S. Models for intestinal fermentation: association between food components, delivery systems, bioavailability and functional interactions in the gut. *Current opinion in biotechnology 18*, 2 (2007), 156–162.

[14] MOLLY, K., WOESTYNE, M. V., AND VERSTRAETE, W. Development of a 5-step multi-chamber reactor as a simulation of the human intestinal microbial ecosystem. *Applied Microbiology and Biotechnology 39*, 2 (1993), 254–258.

[15] MOORTHY, A. S., BROOKS, S. P., KALMOKOFF, M., AND EBERL, H. J. **A spatially continuous model of carbohydrate digestion and transport processes in the colon**. *SUBMITTED.* (2015).

[16] MOORTHY, A. S., AND EBERL, H. J. **Assessing the influence of reactor system design criteria on the performance of model colon fermentation units.** *Journal of bioscience and bioengineering 117*, 4 (2014), 478.

[17] MOORTHY, A. S., AND EBERL, H. J. **compuGUT: An in silico tool for studying flora composition in the human large intestine**, 2015. http://compugut.sourceforge.net.

[18] MUÑOZ-TAMAYO, R. *Mathematical Modelling of Carbohydrate Degradation in the Human Colon*. PhD thesis, UEPSD, INRA, MIA et Universitie Paris-Sud, 2010.

[19] MUÑOZ-TAMAYO, R., LAROCHE, B., WALTER, É., DORÉ, J., AND LECLERC, M. Mathematical modelling of carbohydrate degradation by human colonic microbiota. *Journal of theoretical biology 266*, 1 (2010), 189–201.

[20] PAYNE, A. N., ZIHLER, A., CHASSARD, C., AND LACROIX, C. Advances and perspectives in *in vitro* human gut fermentation modeling. *Trends in biotechnology 30*, 1 (2012), 17–25.

[21] PRESS, W. H., TEUKOLSKY, S. A., VETTERLING, W. T., AND FLANNERY, B. P. Numerical recipes in c: the art of scientific computing, 1992. *Cité en* (1992), 92.

[22] RAMIREZ, I., VOLCKE, E. I., RAJINIKANTH, R., AND STEYER, J.-P. Modeling microbial diversity in anaerobic digestion through an extended adm1 model. *Water research 43*, 11 (2009), 2787–2800.

[23] SADAHIRO, S., OHMURA, T., YAMADA, Y., SAITO, T., AND TAKI, Y. Analysis of length and surface area of each segment of the large intestine according to age, sex and physique. *Surgical and Radiologic Anatomy 14*, 3 (1992), 251–257.

[24] STEWART, E. J., MADDEN, R., PAUL, G., AND TADDEI, F. Aging and death in an organism that reproduces by morphologically symmetric division. *PLoS biology 3*, 2 (2005), e45.

[25] TORTORA, G. J., AND DERRICKSON, B. H. *Principles of anatomy and physiology*. John Wiley & Sons, 2008.

[26] VAVILIN, V., FERNANDEZ, B., PALATSI, J., AND FLOTATS, X. Hydrolysis kinetics in anaerobic degradation of particulate organic material: An overview. *Waste management 28*, 6 (2008), 939–951.

[27] VAVILIN, V., RYTOV, S., AND LOKSHINA, L. Y. A description of hydrolysis kinetics in anaerobic degradation of particulate organic matter. *Bioresource technology 56*, 2 (1996), 229–237.